

1 For submission to Organic Geochemistry

2

3 Title: Comparison of tri-, tetra- and pentacyclic caged hydrocarbons in Australian crude  
4 oils and condensates

5

6 Authors: Alan G. Scarlett<sup>a\*</sup>, Gemma Spaak<sup>a1</sup>, Shifaza Mohamed<sup>b</sup>, Chloé Plet<sup>a2</sup>, Kliti  
7 Grice<sup>a\*</sup>

8

9 <sup>a</sup>Western Australian Organic and Isotope Geochemistry Centre, The Institute for  
10 Geoscience Research, School of Earth and Planetary Sciences, Curtin University,  
11 Western Australia

12 <sup>b</sup> School of Pharmacy and Biomedical Sciences, Curtin University, Western Australia

13

14 \*Corresponding authors: [Alan.Scarlett@curtin.edu.au](mailto:Alan.Scarlett@curtin.edu.au) and [K.Grice@curtin.edu.au](mailto:K.Grice@curtin.edu.au)

15 <sup>1</sup>Present address: Deltares, Subsurface and Groundwater Systems, Daltonlaan 600,  
16 3584 BK Utrecht, the Netherlands

17 <sup>2</sup>Present address: CSIRO Mineral resources, Kensington, WA, 6151, Australia

18

19

20 Abstract

21 Thermally stable and biodegradation resistant, the tricyclic and pentacyclic diamondoid  
22 caged hydrocarbons are commonly used as source and maturity indicators of oils and  
23 potential source-rocks but similar tetracyclic structures appear to have received much  
24 less attention. Using two-dimensional gas chromatography – time of flight mass  
25 spectrometry (GC×GC-TOFMS), 29 Australian crude oils and condensates were  
26 analysed for the presence of caged C<sub>12</sub>H<sub>18</sub> tetracyclics such as ethanoadamantane and  
27 iceane. The thermodynamically more stable 2,4-ethanoadamantane was identified by  
28 comparison with a synthesised authentic standard. Three of its bridgehead methyl-  
29 substituted isomers, 6-methylethanoadamantane (6-ME), 1-ME and 2-ME, were  
30 tentatively assigned based on mass spectral comparison and relative elution order.  
31 Further series of non-bridgehead methyl isomers plus dimethyl isomers were also  
32 inferred based on mass spectra and 2D elution positions. The tri-, tetra and pentacyclic  
33 caged hydrocarbons and their methyl-substituted homologues were semi-quantified in  
34 the Australian oils. The potential of a novel index, the methylethanoadamantane index  
35 (MEI), based on the ratio of the more stable bridgehead isomers divided by the sum of  
36 all the methyl substituted isomers ( $MEI = \frac{\Sigma(6-ME + 1-ME + 2-ME)}{\Sigma Total}$   
37 methylethanoadamantanes), was explored. A significant positive association was found  
38 between the MEI and MAI ( $r^2 = 0.203, p < 0.05$ ) and a significant negative association  
39 was found between MEI and MDI ( $r^2 = 0.246, p < 0.05$ ). Stronger relationships were  
40 found for other commonly applied diamondoid ratio indices including  $\Sigma$  Methyl  
41 Adamantanes/ $\Sigma$  Methyl Diamantanes ( $\Sigma MA/\Sigma MD$ ) versus  $\Sigma MA/\Sigma ME$  ( $r^2 = 0.781,$   
42  $p < 0.0001, n = 26$ ). The relatively low volatility of the ethanoadamantanes compared to  
43 the adamantanes and their likely greater resistance to microbial attack than the  
44 ethyladamantanes may make analysis of these compounds a useful addition to the  
45 commonly measured diamondoids.

46 Keywords: 2,4-cyclopentano-adamantane; diamondoid; GC×GC; synthesis; biomarker;  
47 maturity indicator

48

49 **Highlights**

- 50 • Caged tetracyclic hydrocarbons found in a range of Australian oils and  
51 condensates
- 52 • 2,4-ethanoadamantane synthesised and confirmed as present in samples
- 53 • Concentrations of ethanoadamantane and homologues generally similar to  
54 diamantanes
- 55 • Novel ethanoadamantane indices show correlation with some diamondoid  
56 indices

57

58

59

60

61

62

## 63 1. Introduction

64 Diamondoids are saturated hydrocarbons with cage-like structures that resemble  
65 diamonds. As well as applications in nanotechnology and biomedicine they have been  
66 widely applied in organic geochemistry (reviewed by Mansoori et al., 2012). In  
67 particular, tricyclic and pentacyclic diamondoid hydrocarbons have been used as  
68 maturity and source indicators due to their high thermal stability and resistance to  
69 biodegradation (Chen et al., 1996; Dahl et al., 1999; Grice et al., 2000; Mansoori et al.,  
70 2012; Marchand, 2003; Moldowan et al., 2015; Stout and Douglas, 2004; Wang et al.,  
71 2006), but despite this clear interest in caged hydrocarbons, similar tetracyclic  
72 structures do not appear to have been utilised or indeed routinely reported in crude  
73 oils.

74 Pyrolysis experiments have shown that the lower molecular weight diamondoids i.e. the  
75 tricyclic adamantane (A;  $C_{10}H_{16}$ ) and the pentacyclic diamantane (D;  $C_{14}H_{20}$ ) are  
76 generated early during the formation of oil with destruction later in the cracking process  
77 (Fang et al., 2013). The diamantanes have been reported to be generated at greater  
78 maturity (1.6–2.7% EasyRo) than the adamantanes (1.0–2.3% EasyRo) (Fang et al.,  
79 2013). No similar data concerning the generation of tetracyclic cage structures could be  
80 found in the literature but these may have been formed at the same time. The high  
81 resistance to biodegradation observed for the tri- and pentacyclic structures is likely to  
82 also occur for the caged tetracyclics. The interest in the use of diamondoids as  
83 molecular proxies for determining the thermal maturity of oils and source rocks can be  
84 attributed to the relative differences in the thermal stability of their methyl substituted  
85 isomers (bridgehead substituted have greater stability), and their presence in oils in  
86 which other maturity indicators such as hopanes and methylphenanthrenes are absent  
87 (e.g. Dahl et al., 1999; Grice et al., 2000; Wei et al., 2007b). For example, Dahl et al.  
88 (1999) used variations in the concentrations of 3- + 4-methyldiamantanes within an oil

89 to determine changes in the mass of the oil and to assess the extent of oil cracking.  
90 This was based on the assumption that the mass of 3- + 4-methyldiamantanes  
91 remained constant during cracking. Various indices have also been applied. For  
92 example, Fang et al. (2013) reported that in the generation stage of diamondoids  
93 (<2.0% Easy-Ro), the Methyl Adamantane index (MAI) [= 1-MA/(1-MA + 2-MA)], was  
94 found to be constant suggesting that it may be source dependent as it appeared to be  
95 unaffected by thermal maturation. The authors concluded that MAI together with the  
96 dimethyladamantane indices (see below) are useful for determining the source-region  
97 affinities of oils at the generation stage. Various other indices have been proposed and  
98 used as maturity and oil – source correlation indicators, these include the Methyl  
99 Diamantane Index (MDI) [= 4-MD/(1-MD + 3-MD + 4-MD)], the DiMethyl Diamantane  
100 Index-1 (DMDI-1) [= 4,9-DMD/(4,9-DMD + 3,4-DMD)], and DMDI-2; = [4,9-DMD/ (4,9-  
101 DMD + 4,8-DMD)] (Chen et al., 1996; Zhang et al., 2005). Additional ratios include the  
102 Ethyl Adamantane Index (EAI) [= 1-EA/(1-EA + 2-EA)], the DiMethyladamantane Index  
103 (DMAI-1) [= 1,3-DMA/(1,2-DMA + 1,3-DMA)] and DMAI-2 [= 1,3-DMA/(1,3-DMA + 1,4-  
104 DMA)], and the TriMethyl Adamantane Index (TMAI-1) [= 1,3,5- TMA/(1,3,5-TMA +  
105 1,3,4-TMA)], and TMAI-2 [= 1,3,5- TMA/(1,3,5-TMA + 1,3,6-TMA)] (Grice et al., 2000;  
106 Schulz et al., 2001; Wei et al., 2007b). Ratios based on methyl-substituted to parent  
107 diamondoids e.g. MA/A [(1-MA + 2MA)/A] (Wingert, 1992) and ratios of tri- to  
108 pentacyclic structures e.g. A/D (Fang et al., 2013) have also been used. There does  
109 not however appear to be any indices based on tetracyclic caged hydrocarbons.

110 There are 5291 possible isomers for the tetracyclic structures of C<sub>12</sub>H<sub>18</sub> hydrocarbons  
111 with 12 skeletal carbon atoms (Cupas and Hodakows, 1974), of which few are stable.  
112 One such is Tetracyclo[5.3.1.1<sup>2,6</sup>.0<sup>4,9</sup>]dodecane (iceane; Fig. S1) which can be  
113 visualised as two chair cyclohexanes connected by three axial bonds (Cupas and  
114 Hodakows, 1974). The trivial name iceane was coined by Fieser (cited by Cupas and

115 Hodakows, 1974) due to its structure being the geometrical hydrocarbon analog of  
116 crystalline water. Iceane was synthesised in the 1970s (Hamon and Taylor, 1975;  
117 Hamon and Taylor, 1976) and its crystal structure determined by X-ray diffraction  
118 (Hamon et al., 1977). However, iceane is not the most stable isomer due to the strain  
119 energy of *ca* 25 kcal/mole resulting from the three flagpole-flagpole interactions  
120 (Farcasiu et al., 1974). The less symmetrical non-diamondoid structure  
121 tetracyclo[6.3.1.0<sup>2,6</sup>.0<sup>5,10</sup>]dodecane (2,4-ethanoadamantane; Fig. 1, Fig. S1) is reported  
122 to be 6-7 kcal/mole more stable than iceane which also possesses unfavourable  
123 entropy resulting from its high symmetry (Farcasiu et al., 1974). Of all the possible  
124 tetracyclic caged hydrocarbons, the most stable ethanoadamantanes and iceanes are  
125 most likely to persist during the cracking process (Osawa et al., 1980).

126 If ethanoadamantanes and/or iceanes are present and widespread in oils and  
127 condensates they could assist with source correlation and provide either additional  
128 information or help to confirm thermal maturity in conjunction with other indices. For  
129 example, the low molecular weight adamantanes are quite volatile and may be lost *via*  
130 evaporation at any stage from before the sample is collected to the point at which it is  
131 analysed (Li et al., 2012). Hence, where the only diamondoids present are tricyclic  
132 adamantanes, having an additional class of compound for reference could be useful as  
133 evaporative losses may affect maturity indices. In this preliminary study, we first  
134 searched for tetracyclic caged hydrocarbons (molecular ion, M<sup>+</sup> 162) and their methyl  
135 substituted isomers (M<sup>+</sup> 176 and M<sup>+</sup> - CH<sub>3</sub> *m/z* 161) in a commercial mixture of  
136 alkyldiamantanes derived from gas condensate (PolyDiamond Technologies,  
137 Pleasanton, CA). This commercial mixture also contained much smaller quantities of  
138 adamantanes, triamantanes and tetramantanes, as this was a relatively simple mixture  
139 that was free from interferences typically associated with oil analysis. To reduce the  
140 complexity further, we applied comprehensive two dimensional gas chromatography

141 with time of flight mass spectrometry (GC×GC-TOFMS) which has previously been  
142 used very successfully to analyse diamondoid hydrocarbons in oils (e.g. Li et al., 2012;  
143 Silva et al., 2013; Silva et al., 2011; Tran et al., 2010). As neither iceane nor 2,4-  
144 ethanoadamantane were readily available commercially, the latter was synthesised  
145 using a synthetic protocol previously reported in the literature (Farcasiu et al., 1974;  
146 Osawa et al., 1980). Following tentative assignment of peaks present in the  
147 alkyldiamantane mixture, their two dimensional (2D) retention times and time of flight  
148 mass spectra were used to investigate 29 Australian crude oils and condensates.  
149 Compounds were quantified based on concentration response curves of reference  
150 standards of adamantane and diamantane.

151

## 152 **2. Material and Methods**

### 153 *2.1 Standards*

154 Diamantane (≥99 % purity) and the alkyldiamantane mixture (≥98 % purity, also  
155 containing additional diamondoids including adamantanes, triamantanes and  
156 tetramantanes) were supplied by PolyDiamond Technologies (Pleasanton, CA).  
157 Adamantane (≥99%) was supplied by Sigma-Aldrich (Sydney, Australia). Solvents were  
158 Reagent grade supplied by Honeywell International Inc, Muskegon, MI, USA.

### 159 *2.2 Synthesis of 2,4-ethanoadamantane*

160 Starting materials for the synthesis of 2,4-ethanoadamantane was obtained from  
161 Sigma-Aldrich (Sydney, Australia) and used without further purification. Organic  
162 solvents used in the reactions were dried prior to performing the reaction. Flash  
163 chromatography was conducted using Merck silica gel 60 µm. Reactions were  
164 monitored by thin layer chromatography using Merck silica gel 60 µm TLC plates with  
165 aluminium backing and containing F254 fluorescent indicator. Compounds were

166 visualized on the TLC plate using potassium permanganate solution containing  $\text{KMnO}_4$   
167 (1.5 g),  $\text{K}_2\text{CO}_3$  (10 g), 10% NaOH solution (1.25 mL) diluted to 200 mL with deionised  
168 water. NMR spectra were collected using a Bruker Ultraspin 400 MHz spectrometer ( $^1\text{H}$   
169 400 MHz;  $^{13}\text{C}$  100 MHz).

170 The synthesis of 2,4-ethanoadamantane (tetracyclo[6.3.1.0]dodecane) **6** was carried  
171 out as described in Fig. 1. The intermolecular Diels-Alder reaction of  $\alpha$ -pyrone **1** and  
172 *cis,cis*-1,5-cyclooctadiene **2** resulted in the *cis*-bicyclo[6.4.0]dodeca-4,9,11-triene **3**.  
173 The intermediate **3** cyclizes *via* an intramolecular Diels-Alder reaction to yield  
174 tetracyclo[6.4.0.0.0]dodec-10-ene **4** in 60% yield. The subsequent hydrogenation of  
175 compound **4** yielded tetracyclo[6.4.0.0.0]dodecane **5** in excellent yield. 2,4-  
176 ethanoadamantane **6** was then conveniently prepared by the Lewis acid catalysed  
177 isomerization of compound **5**. The identity of compound **6** was confirmed by NMR  
178 spectroscopy and mass spectral comparison (Fig. 1, Fig. S4). Further details of the  
179 synthesis method are supplied in Supplementary Information.

### 180 2.3 Samples

181 Crude oils and condensates were supplied by Geoscience Australia or were available  
182 from a previous study (Grice et al., 2000). Basic information concerning the properties  
183 of the samples are presented in Table 1 and Fig. S2. Further information is available  
184 from previous studies (Alexander et al., 1983; Edwards and Zumberge, 2005; Grice et  
185 al., 2000; Palu et al., 2017; Spaak, 2017; Spaak et al., 2016; Volkman et al., 1983). To  
186 minimise evaporative losses, the samples were analysed as *n*-hexane-soluble fractions  
187 of whole crude oils and condensates. To check for possible interferences from aromatic  
188 compounds, the Carnarvon oils were also fractionated by silica gel chromatography to  
189 produce a 'Saturated' (*n*-hexane elution) and 'Aromatic' (7:3 *n*-hexane:dichloromethane  
190 elution) fraction. Additional oils from older sources and outside of the Australian region



191 were also checked for the presence/absence of the of C<sub>12</sub>H<sub>18</sub> tetracyclic hydrocarbons  
192 but were not quantified.

#### 193 2.4 GC×GC-TOFMS analysis

194 The *n*-hexane-soluble fractions of whole oils and condensates plus saturated and  
195 aromatic fractions were analysed using a Leco Pegasus IV system equipped with dual  
196 stage cryogenic modulator (Leco, Saint Joseph, MI, USA). For all samples the primary  
197 column was a 60 m × 0.25 mm × 0.25 μm Rxi 5Sil MS (Restek, Bellefonte, PA, USA).  
198 For the Carnarvon and Gippsland oils the primary column was coupled to a secondary  
199 1.4 m × 0.25 mm × 0.25 μm DB-17ms (Agilent) column (Set-1). For the remaining oils  
200 and condensates, the secondary column was a 1.3 m × 0.18 mm × 0.18 μm RXi-17MS  
201 (Restek) (Set-2). Adamantane, diamantane, and the alkyldiamantane mixture plus a  
202 subset of the Browse oils and condensates were analysed on both column sets to  
203 ensure consistent results. The carrier gas was ultrahigh purity helium with constant flow  
204 of 2 mL min<sup>-1</sup> for Set-1 and 1 mL min<sup>-1</sup> for Set-2. The inlet temperature was 310 °C with  
205 1 μL injection. For Set-1 the conditions were: 40 °C (1 min isothermal), then 3 °C min<sup>-1</sup>  
206 to 320 °C, (isothermal 30 min) and a modulation period of 3 s, with secondary oven  
207 offset of 1 °C and modulator offset 15 °C. For Set-2, the conditions were: 50 °C (1 min  
208 isothermal), then 2.5 °C min<sup>-1</sup> to 200 °C then 20 °C min<sup>-1</sup> to 320 °C, (isothermal 10  
209 min) with a modulation period of 4 s, with secondary oven offset 5 °C and modulator  
210 offset 15 °C. The mass spectrometer electron ionisation was 70 eV; the ion source  
211 temperature was 250 °C and the transfer line 320 °C. The scan speed was 100 Hz with  
212 a range of 45–580 Daltons (Da). ChromaTOF (LECO) software package was used for  
213 instrument control and data analysis. Minimum acceptable signal to noise ratio was  
214 30:1. Coefficient of variation for triplicate analyses of lowest concentrations of  
215 standards (0.25 μg mL<sup>-1</sup>) was <3%. Mass spectra were compared with National

216 Institute of Standards & Technology (NIST, Gaithersburg, MD, USA) libraries plus in-  
217 house TOFMS libraries.

#### 218 2.4 Semi-quantification of tri-, tetra- and pentacyclic caged hydrocarbons

219 Adamantanes and diamantanes were quantified using external calibration curves of  
220 adamantane and diamantane. Linear concentration response curves ( $r^2 > 0.99$ ) were  
221 generated from seven concentrations ranging from  $0.25 \mu\text{g mL}^{-1}$  to  $50 \mu\text{g mL}^{-1}$ . Peak  
222 areas were calculated from the respective base peaks. The external calibration curves  
223 were determined daily and selected standard concentrations were analysed after every  
224 fourth sample to account for any variation throughout the sample sequence. As  
225 ethanoadamantane was not available in pure crystalline form for quantification, the  
226 peaks assigned as tetracyclic caged structures were semi-quantified based on the  
227 linear concentration response curves of adamantane and diamantane standards which  
228 gave very similar concentrations.

#### 229 2.5 Molecular properties computation

230 Molecular properties and energies were computed using Spartan '16 version 2.0.7  
231 (Wavefunction Inc, Irvine, CA). Strain energies were calculated using the program  
232 settings 'Molecular mechanics'; total energies and thermodynamic properties were  
233 calculated using 'Equilibrium Geometry' at ground state with 'Density Functional'  
234  $\omega\text{B97X-D}$  and 6-31G\*.

235

### 236 3. Results and Discussion

#### 237 3.1 Chromatography and peak assignment of alkyldiamantane mixture

238 The orthogonal nature of GC $\times$ GC results in ordered chromatograms in which  
239 relationships between molecules in terms of carbon number and polarity are easily

240 visualised. Analysis of the alkyldiamantane mixture revealed a clear linear relationship  
241 between the carbon number of diamondoids and their 2D elution positions (Fig. 2). A  
242 peak eluting midway between adamantane and diamantane, and between  $nC_{13}$  and  
243  $nC_{14}$  (Kovats Index for DB5 column (on GC×GC) = 1363.0), was found to have a  
244 basepeak and  $M^+$  of  $m/z$  162 consistent with a  $C_{12}$  tetracyclic hydrocarbon (Fig. S3  
245 peak i and Fig. S4A). The mass spectrum of this peak was very similar to that of iceane  
246 (NIST library, Fig. S4B). However, the mass spectrum of the thermodynamically more  
247 stable ethanoadamantane, isolated from Hodonin oil (Czechoslovakia) reported over  
248 50 years ago (Hála et al., 1966), was also similar although the relative intensity of the  
249 fragment ions were generally lower (Fig. S4C). As authentic standards of iceane and  
250 ethanoadamantane were not available, we synthesised the latter (as this was the most  
251 likely candidate due to its thermodynamic stability) in order to ascertain which  $C_{12}$   
252 tetracyclic hydrocarbon was present. The synthesised 2,4-ethanoadamantane eluted at  
253 the same apolar and polar retention times as the tentatively assigned  $C_{12}H_{18}$  tetracyclic  
254 hydrocarbon and possessed an identical mass spectrum and we were therefore able to  
255 unambiguously assign the  $m/z$  162 peak as 2,4-ethanoadamantane (Fig. 1 and 3). As  
256 only one peak with molecular ion  $m/z$  162 was present, iceane was concluded not to be  
257 present.

258 Eluting just before in the second dimension, i.e. less polar, the ethanoadamantane  
259 peak were three peaks with basepeak  $m/z$  161 and molecular ion  $m/z$  176 ( $C_{13}H_{20}$ ),  
260 consistent with methyl substituted  $C_{12}$  tetracyclic hydrocarbons (Fig. S5 corresponding  
261 to peaks ii – iv in Fig. S3). Due to the symmetry of iceane, only two methyl substituted  
262 isomers are possible with one substituted on the thermally more stable bridgehead  
263 carbon (Fig. S1, Table S1). No library mass spectra for methyl iceanes were available  
264 for comparison. With less symmetry than iceane, ethanoadamantane can have multiple  
265 methyl substitutions including four possible bridgehead substituted structures (Fig. S1),

266 although it was previously reported that 8-methylethanoadamantane could not be  
267 synthesised *via* bromination of 2,4-ethanoadamantane (Osawa et al., 1980).  
268 Comparison of the mass spectra for 1-, 6- and 2-methylethanoadamantanes reported  
269 by Osawa et al. (1980) with the three peaks in the alkyldiamantane mixture (Fig. S6  
270 and S7), revealed reasonable matches for 1- and 6-methylethanoadamantane for the  
271 first two eluting peaks (ii and iii) respectively although the mass spectra of these two  
272 peaks are very similar. Based on the elution order and relative intensities of the base  
273 peaks  $m/z$  161 to  $m/z$  176 reported by Osawa et al. (1980), the first eluting peak (ii)  
274 should be 1-methylethanoadamantane and second (iii) 6-methylethanoadamantane  
275 (Fig. S3 and S5A). However, the methylethanoadamantanes were previously analysed  
276 (Osawa et al., 1980) using a different column configuration (highly polar  
277 Nitroterephthalic acid modified polyethylene glycol capillary (FFAP) column compared  
278 to the non-polar Phenyl Arylene polymer (virtually equivalent to a (5%-Phenyl)-  
279 methylpolysiloxane) DB5 in the current study) and different types of mass  
280 spectrometers were used. Hence, the peak assignment must be considered tentative.  
281 For methyl-substituted adamantanes and diamantanes, the most stable isomer elutes  
282 first on non-polar capillary columns but this is not necessarily the case for  
283 methylethanoadamantanes. The second eluting peak (peak iii Fig. S3 and S5B) was  
284 the most abundant as might be expected for the most stable isomer present in  
285 relatively mature oils and condensates. The reported mass spectrum for 2-  
286 methylethanoadamantane (Osawa et al., 1980) showed a molecular ion of  $m/z$  176 that  
287 was more abundant than that of  $m/z$  161; the reverse was true for the third eluting peak  
288 (iv) in the alkyldiamantane mixture (Fig. S6 and S5). In the alkyldiamantane mixture we  
289 therefore assign the peak (i) with  $M^+$  162 as 2,4-ethanoadamantane and tentatively  
290 assign the first two eluting peaks with  $M^+$  176, as 1- and 6-methylethanoadamantane  
291 respectively. The third in the series and least abundant peak in the alkyldiamantane  
292 mixture could either be the fourth bridgehead substituted isomer 8-

293 methylethanoadamantane or possibly a less stable non-bridgehead substituted isomer.  
294 The 2D elution region for the tentatively assigned ethanoadamantane peaks is also that  
295 of alkylbenzenes. However, there was no evidence to suggest that any aromatic  
296 hydrocarbons or heterocyclic compounds were present in the alkyldiamantane mixture.  
297 The third C<sub>13</sub>H<sub>20</sub> peak in the alkyldiamantane mixture (peak iv Fig. S3 and S5C) could  
298 therefore not be assigned. Additional peaks with elution positions and mass spectra  
299 consistent with dimethylethanoadamantanes were also present in low abundance.

### 300 *3.2 Peak assignment of Australian oils and condensates*

301 Having recorded the 2D elution times of 2,4-ethanoadamantane plus the tentatively  
302 assigned peaks corresponding to the methyl-substituted homologues and obtained  
303 GC×GC-TOFMS mass spectra, a range of Australian crude oils and condensates were  
304 assessed. Peaks matching the elution times and mass spectra were present for 2,4-  
305 ethanoadamantane and the tentatively assigned 1- and 6-methylethanoadamantanes  
306 in most of the oils analysed. Interestingly, many oils also contained an additional peak  
307 eluting at the same time (within the modulation period) as the unassigned peak in the  
308 alkyldiamantane mixture but with mass spectra more closely matching that reported by  
309 Osawa et al. (1980) for 2-methylethanoadamantane (Fig. S6). The main difference  
310 being more intense *m/z* 79 and 91 ions in the TOF mass spectrum of the peak within  
311 the oils compared to the reported quadrupole mass spectrum (Fig. S6) as also  
312 observed for the parent compound (Fig. 1). As the oils and condensates had been  
313 analysed as *n*-hexane-soluble fractions of whole oils to minimise losses for  
314 quantification purposes, there was however a possibility of interferences from  
315 alkylbenzenes. The oils were therefore subject to silica gel chromatography to  
316 fractionate them into saturate and aromatic fractions. All of the peaks attributed to  
317 caged tetracyclic hydrocarbons were present only in the saturated fraction.  
318 Alkylbenzenes containing the same fragment ions as the tetracyclic hydrocarbons i.e.

319  $m/z$  91, 105, 119, 133 were present in the aromatic fraction of some of the oils close to,  
320 but not at exactly the same elution times as, the assigned peaks. We therefore  
321 tentatively assigned this additional peak with molecular ion  $m/z$  176 as  
322 2-methylethanoadamantane and rejected the possibility of major interferences from  
323 alkylbenzenes. To check that the assigned peaks were not just an Australian oils  
324 phenomena or restricted to a limited range of reservoir age, some additional oils,  
325 including non-Australian and older reservoirs, were analysed and all were found to  
326 contain at least one of the tentatively identified compounds thus suggesting that they  
327 are common and therefore may have universal application (data not shown).

328

### 329 *3.3 Semi-quantification of Australian oils and condensates*

330 The assigned peaks were semi-quantified based on external calibration curves of  
331 adamantane and diamantane standards. These produced the same or very similar  
332 calculated concentrations and therefore an average was taken where a small  
333 difference occurred. For all of the oils analysed, the concentrations of the tentatively  
334 identified ethanoadamantane were less than that of adamantane but typically similar to  
335 that of the diamantane (Table S2 and Fig. S7). For two oils, Caswell-1 and Caswell-2,  
336 both ethanoadamantane and diamantane were absent (Table S2). Both of these oils  
337 are non-biodegraded but cluster with other Cretaceous oils of the Browse basin (Family  
338 IV, Table 1, Fig. S2). The highest concentrations of ethanoadamantane (up to 859  
339 ppm) were recorded in the same family (IV) but were biodegraded (Tables 1 and S2,  
340 Fig. S2). For the light Rough Range oil, originating from Australia's first bore in 1953 in  
341 the Carnarvon basin, 2,4-ethanoadamantane was present at low abundance (7 ppm)  
342 but diamantane was not observed (Table S2). Of the methyl substituted isomers, the  
343 second eluting peak, tentatively assigned as 6-methylethanoadamantane, was  
344 consistently the most abundant despite the crude oils and condensates possessing a

345 range of maturities and levels of biodegradation (Tables 1 and S2). Generally, the  
346 concentrations of the tentatively identified methylethanoadamantanes relative to the  
347 parent structure showed a similar pattern to that of the diamondoids (Table S2, Fig.  
348 S7). This is explored further in section 3.5.

349 The high resistance to biodegradation observed for the tri- and pentacyclic  
350 diamondoids, appears to also apply for the tetracyclics. Although concentrations vary  
351 considerably (Table S2) for the two most biodegraded oils, Mardie (Peter and  
352 Moldowan (P&M; scale 8 (Peters et al., 2007)) and Lakes Entrance (P&M scale 7)  
353 (Grice et al., 2000; Volkman et al., 1983), this is likely source-related as the former is  
354 from the Carnarvon basin and the latter from Gippsland basin (Tables 1 and S2). Both  
355 of these oils contained lower concentrations of diamondoids in general compared to the  
356 biodegraded Cretaceous oils of the Browse basin and less than the light Jurassic  
357 Montara oil from the Bonaparte basin (Table S2 and Fig. S7).

358

#### 359 *3.4 Fate of ethanoadamantanes and diamondoids*

360 Despite the recalcitrant nature of the diamondoids, biodegradation does appear to  
361 occur as evidenced by the presence of their corresponding carboxylic acids discovered  
362 in oil sands process-affected waters (OSPW) derived from the oil extraction industry in  
363 Alberta Canada (Rowland et al., 2011a; Rowland et al., 2011b). Similarly there is  
364 evidence for biodegradation of the alkylsubstituted homologues of ethanoadamantane  
365 to their corresponding carboxylic acids (Wilde and Rowland, 2018). By converting the  
366 acids extracted from OSPW to hydrocarbons, Wilde and Rowland (2018) not only  
367 confirmed the presence of numerous tri- and pentacyclic diamondoid acids, they also  
368 tentatively assigned several peaks as “alkyl 2,4-cyclopentano-adamantanes” i.e.  
369 alkylated ethanoadamantanes and by inference their corresponding carboxylic acids.

370 Mass spectra obtained by GC×GC-TOFMS assigned by Wilde and Rowland (2018) as  
371 methyl, dimethyl and trimethyl substituted ethanoadamantane closely matched mass  
372 spectra observed in the oils reported herein. Peaks with mass spectra consistent with  
373 higher degrees of alkylation were most prominent in biodegraded Cretaceous oils from  
374 the Browse basin e.g. Cornea-1 (Fig.3 and Fig. S8). A study of the relative abundance  
375 of the ethanoadamantane acids compared to the diamondoid acids might prove  
376 informative e.g. when interpreting diamondoid indices.

377

### 378 *3.5 Comparison of ethanoadamantane and diamondoid indices*

379 The diamondoid indices MAI and MDI have been widely applied (e.g. Chen et al., 1996;  
380 Fang et al., 2013; Grice et al., 2000; Li et al., 2000; Li et al., 2012; Schulz et al., 2001;  
381 Wang et al., 2006; Wei et al., 2007a; Wei et al., 2007b) but some limitations seem to  
382 apply. For example, MDI was found not to be a useful maturity parameter for over-  
383 mature carbonate-rich source rocks (>2.0% Ro) (Li et al., 2000). The MAI may be  
384 compromised due to evaporative processes affecting the lower molecular weight  
385 compounds (Li et al., 2012). Having additional indices to help corroborate the MAI or  
386 MDI may therefore be useful or may highlight unusual samples. However, the  
387 diamondoid indices are based on the relative concentrations of bridgehead to total  
388 methyl isomers whereas our study has only tentatively assigned bridgehead isomers.  
389 Many of the samples also possessed additional peaks eluting later in the apolar  
390 primary dimension with base peak or prominent fragment ions  $m/z$  161 and  $M^+$  176  
391 (Fig. 3 and Fig. S8). These tended to be more prominent in biodegraded oils such as  
392 Lakes Entrance and Cornea-1. These are likely to be non-bridgehead  
393 methylethanoadamantanes but further research would be required to unambiguously  
394 confirm this. As diamondoid indices tend to be applied in the absence of other maturity  
395 or source indicators, the limited presence of these additional peaks in non-biodegraded



396 oils may not be problem. Within our sample set, 24 of the oils and condensates  
397 possessed at least some of these additional methylethanoadamantanes, so we  
398 hypothesised that a relationship might exist related to their thermal stability. We  
399 therefore explored the potential of a novel index, the methylethanoadamantane index  
400 (MEI) based on the same thermal stability rationale as MAI and MDI. For the MEI, this  
401 is the ratio of the combined peak areas of the three stable bridgehead isomers i.e. 6-  
402 methylethanoadamantane (6-ME) + 1-ME + 2-ME divided by the sum of peak areas for  
403 all methyl substituted isomers present ( $\Sigma$ Total ME; Equation 1).

404 Equation 1:  $MEI = \Sigma(6-ME + 1-ME + 2-ME) / \Sigma$ Total ME

405 Combining data from 24 crude oils and condensates regardless of basin, reservoir or  
406 biodegradation status (including only peaks with acceptable mass spectra and elution  
407 times) allowed linear regression to be performed on a reasonable sized dataset to test  
408 for association between the MEI and the equivalent diamondoid indices (Table 2). A  
409 significant positive association was found between the MEI and MAI ( $r^2 = 0.203$ ,  
410  $p < 0.05$ ) and a significant negative association was found between MEI and MDI ( $r^2 =$   
411  $0.246$   $p < 0.05$ ). This suggests that the MEI could be used as a substitute for MAI if  
412 water washing or evaporative losses were suspected.

413 Fang et al. (2013) reported that the ratios A/D and MA/MD increase with increasing  
414 thermal maturity in the range 1.0–2.0% EasyRo, suggesting that these diamondoid  
415 concentration ratios can be used to assess the thermal maturity of oils at this maturity  
416 stage. Using the combined dataset of Australian oils with acceptable criteria (Table 2),  
417 it was found that there was a significant association between A/D and the ratio  
418 Ethanoadamantane/Diamantane (E/D) with  $r^2$  of 0.204 ( $p < 0.05$ ,  $n = 26$ ) and a stronger  
419 association between A/D and A/E with  $r^2$  of 0.460 ( $p < 0.0005$ ,  $n = 26$ ). Even stronger  
420 associations were found for the methyl isomer versions of these ratios: the linear  
421 regression of  $\Sigma$ MA/ $\Sigma$ MD and  $\Sigma$ ME/ $\Sigma$ MD had  $r^2$  of 0.287 ( $p < 0.005$ ,  $n = 26$ ) and

422  $\Sigma\text{MA}/\Sigma\text{ME}$  had  $r^2 = 0.781$  ( $p < 0.0001$ ,  $n = 26$ ; Fig. 4). For all of the plots, there were  
423 some noticeable deviations from the regression line of fit, e.g. for the regression of all  
424 oils for  $\Sigma\text{MA}/\Sigma\text{MD}$  versus  $\Sigma\text{MA}/\Sigma\text{ME}$ , Tuna-4 showed considerable deviation from the  
425 linear regression line whereas the biodegraded Lakes Entrance oil, from the same  
426 basin, plotted very close to the line (Fig. 4). As these deviations may be related to  
427 either the reservoir age, basin or their biodegradation level, the relationships between  
428 ratios were explored further based on previously established grouping of the oils and  
429 condensates (Alexander et al., 1983; Edwards et al., 2016; Edwards and Zumberge,  
430 2005; Grice et al., 2000; Palu et al., 2017; Volkman et al., 1983).

431 From assessing the data based on hierarchical cluster analysis reported for families of  
432 oils and condensates shown in Fig. S2 (Edwards et al., 2016; Palu et al., 2017), it was  
433 found that only family IV did not show a significant relationship ( $r^2 = 0.472$ ,  $p = 0.2$ ,  $n =$   
434 5) between  $\Sigma\text{MA}/\Sigma\text{MD}$  and  $\Sigma\text{MA}/\Sigma\text{ME}$  (Table 2). The regression excluded the light  
435 non-biodegraded oils from the Caswell field as only the five biodegraded oils from this  
436 Cretaceous family (Table 1) contained ethanoadamantanes and diamantanes  
437 suggesting that biodegradation may influence the relationship. However, the Carnarvon  
438 oils, containing the heavily biodegraded Mardie crude oil, light oils e.g. Barrow and  
439 mixtures (Table 1), showed a strong positive linear relationship for this ratio ( $r^2 = 0.881$ ,  
440  $p < 0.01$ ,  $n = 6$ ) despite the range in biodegradation status suggesting that this is not a  
441 major factor. Clearly there are many aspects that may affect biomarker and other  
442 indicator ratios so more research is required to tease out possible influences on the  
443 concentrations and ratios reported in this preliminary study.

### 444 *3.6 Potential uses and future work*

445 The relatively low volatility of the ethanoadamantanes compared to the adamantanes  
446 may provide a useful check on indices based on the latter. Although the ethyl  
447 substituted adamantanes, which have a similar molecular weight (164 Da as

448 ethanoadamantane (162 Da), are less volatile than the methyladamantanes they are  
449 more likely to be affected by biodegradation due to the exposed ethyl group and hence,  
450 the use of the Ethyl Adamantane Index (EAI) as an alternative to the MAI maturity  
451 indicator is problematic. For example, the oils of the Carnarvon basin were found to  
452 have reasonably similar MAI, consistent with a previous study (Grice et al., 2000), as  
453 expected for maturity indicators unaffected by biodegradation but calculation of EAI  
454 revealed a high degree of variation between light, heavy biodegraded and mixed oils  
455 e.g. Barrow 19%, Mardie 74% and Windalia 39% (Table 2). Also, in situations where  
456 diamantanes are absent, the ethanoadamantanes could be used as a substitute given  
457 their close association with diamantane and methyladamantane concentrations (Table  
458 2, S2, Fig. 4). Ideally, future studies could unambiguously confirm the identity of the  
459 less stable non-bridgehead methylethanoadamantanes which will improve the MEI  
460 which could then be applied to a larger selection of oils with a greater range of  
461 maturities.

462 At present, despite increasing popularity, the availability of GC×GC-TOFMS is still  
463 limited compared to GC-MS. However, analysis of the current samples by GC-MS in  
464 full-scan mode produced unresolved complex mixtures in many of the oils. To test if  
465 2,4-ethanoadamantane and the tentatively assigned methyl-substituted isomers could  
466 be detected using GC-MS selected ion monitoring (SIM), the alkyldiamantane mixture  
467 plus both a saturates only and a combined saturates and aromatics fraction of the  
468 biodegraded Lakes Entrance crude oil were analysed using a SIM method (Fig. S9).  
469 Although both the parent and methyl isomers could be detected in all the analyses,  
470 care would need to be taken if aromatics were present due to the similarities of  
471 alkylbenzene mass spectra and the elution time window. Due to their alkyl chain,  
472 alkylbenzenes can elute with the saturated fraction during commonly used fractionation

473 procedures so it is recommended that protocols are checked to ensure that pure  
474 saturates fractions are obtained in order to reduce the risk of misidentification of peaks.

475 Analyses of source rocks was outside the scope of this study. Further research could  
476 be focused on the relative concentrations of ethanoadamantanes in rocks of varying  
477 maturity and possibly pyrolysis experiments (*sensu* Fang et al., 2013) to ascertain  
478 when these compounds are generated.

479

#### 480 **4. Conclusions**

481 This study has for the first time identified and semi-quantified the C<sub>12</sub>H<sub>18</sub> caged  
482 hydrocarbon 2,4-ethanoadamantane and tentatively assigned three of its  
483 methyl-substituted isomers in a range of Australian crude oils and condensates. Peaks  
484 consistent with additional methyl and dimethyl substituted homologues were also  
485 observed. Like the diamondoids, these tetracyclic structures appear to be highly  
486 resistant but not immune to biodegradation. Concentrations of these compounds were  
487 generally similar to that of the pentacyclic diamondoids (diamantanes) producing  
488 significant linear relationships between A/D and A/E, and also the equivalent methyl  
489 isomer ratios. A novel ratio, MEI, based on the relative thermal stabilities of the  
490 methylethanoadamantanes showed statistically significant relationships ( $p < 0.05$ ) with  
491 diamondoid maturity indices. The relatively lower volatility of ethanoadamantanes  
492 compared to adamantanes in conjunction with their resistance to microbial attack make  
493 these tetracyclic structures suitable for studies where evaporative losses and  
494 biodegradation are an issue. Measurement of ethanoadamantane and its alkylated  
495 homologues in conjuncture with the commonly applied diamondoids may therefore  
496 prove useful for oil-source correlations and maturity studies but further investigation of  
497 a wider range of samples is necessary.

498 **Acknowledgements**

499 We thank WA-OIGC for funding Alan Scarlett. Chloe Plet was supported by ARC  
500 linkage grant LP150100341. Gemma Spaak was supported by an ARC DORA grant  
501 (DP13010057). ARC is acknowledged for ARC LE130100145 for GC×GC-TOFMS. We  
502 thank Geoscience Australia for the supply of the Browse basin oils. We also thank Alan  
503 Payne, School of Molecular and Life Sciences at Curtin University for his helpful  
504 discussions related to the synthesis of 2,4-ethanoadamantane. In addition, we thank  
505 the anonymous reviewers for their helpful comments and suggestions.

506 **Supporting information**

507 Additional synthesis method details and NMR spectra; molecular properties of tri-,  
508 tetra- and pentacyclic caged hydrocarbons; concentrations of ethanoadamantanes and  
509 diamondoids in crude oils and condensates; comparative chemical structures of iceane  
510 and 2,4-ethanoadamantane with carbon position numbers; dendrogram comparing  
511 Basin fluid families; GC×GC-TOFMS chromatograms of elution region of tetracyclic  
512 caged hydrocarbon peaks referred to in text with associated mass spectra; a clustered  
513 barchart giving an overview of concentrations; and a GC-MS SIM chromatogram of the  
514 ethanoadamantanes and diamantanes.

515 **References**

- 516 Alexander, R., Kagi, R.I., Woodhouse, G.W., Volkman, J.K., 1983. The geochemistry of some  
517 biodegraded australian oils. The APPEA Journal 23, 53-63.
- 518 Chen, J.H., Fu, J.M., Sheng, G.Y., Liu, D.H., Zhang, J.J., 1996. Diamondoid hydrocarbon ratios:  
519 Novel maturity indices for highly mature crude oils. Organic Geochemistry 25, 179-190.
- 520 Cupas, C.A., Hodakows, L., 1974. ICEANE. Journal of the American Chemical Society 96, 4668-  
521 4669.
- 522 Dahl, J.E., Moldowan, J.M., Peters, K.E., Claypool, G.E., Rooney, M.A., Michael, G.E., Mello,  
523 M.R., Kohnen, M.L., 1999. Diamondoid hydrocarbons as indicators of natural oil  
524 cracking. Nature 399, 54-57.
- 525 Edwards, D.S., Grosjean, E., Palu, T., Rollet, N., Hall, L., Boreham, C.J., Zumberge, A., Zumberge,  
526 J.E., Murray, A.P., Palatty, P., Jinadasa, N., Khider, K., Buckler, T., 2016. Geochemistry  
527 of dew point petroleum systems, Browse Basin, Australia. In: Proceedings Australian  
528 Organic Geochemistry Conference, Fremantle, 4-7, December 2016.  
529 <http://www.ga.gov.au/metadata-gateway/metadata/record/101720>.
- 530 Edwards, D.S., Zumberge, J.E., 2005. The Oils of Western Australia. Petroleum Geochemistry  
531 and Correlation of Crude Oils and Condensates from Western Australia and Papua New  
532 Guinea, Geoscience Australia and GeoMark Research Ltd unpublished report, Canberra  
533 and Houston, GeoCat 37512.
- 534 Fang, C.C., Xiong, Y.Q., Li, Y., Chen, Y., Liu, J.Z., Zhang, H.Z., Adedosu, T.A., Peng, P.A., 2013. The  
535 origin and evolution of adamantanes and diamantanes in petroleum. Geochim.  
536 Cosmochim. Acta 120, 109-120.
- 537 Farcasiu, D., Wiskott, E., Osawa, E., Thieleck, W., Engler, E.M., Slutsky, J., Schleyer, P.V., 1974.  
538 Ethanoadamantane - most stable C<sub>12</sub>H<sub>18</sub> isomer. J. Am. Chem. Soc. 96, 4669-4671.

539 Grice, K., Alexander, R., Kagi, R.I., 2000. Diamondoid hydrocarbon ratios as indicators of  
540 biodegradation in Australian crude oils. *Organic Geochemistry* 31, 67-73.

541 Hála, S., Landa, S., Hanuš, V., 1966. Isolation of Tetracyclo[6.3.1.0<sup>2,6</sup>.0<sup>5,10</sup>]dodecane and  
542 Pentacyclo[7.3.1.1.4.12.0<sup>2,7</sup>.0<sup>6,11</sup>]tetradecane (Diamantane) from Petroleum.  
543 *Angewandte Chemie International Edition in English* 5, 1045-1046.

544 Hamon, D., Raston, C., Taylor, G., Varghese, J., White, A., 1977. Crystal structure of  
545 Tetracyclo[5.3.1.12.6.0<sup>4,9</sup>]dodecane (iceane). *Aust. J. Chem.* 30, 1837-1840.

546 Hamon, D.P.G., Taylor, G.F., 1975. A synthesis of tetracyclo [5.3.1.12,6<sup>04,9</sup>] dodecane (iceane).  
547 *Tetrahedron Lett.* 16, 155-158.

548 Hamon, D.P.G., Taylor, G.F., 1976. Synthesis of tetracyclo 5,3,1,1(2,6),0(4,9) dodecane (iceane).  
549 *Aust. J. Chem.* 29, 1721-1734.

550 Li, J.G., Philp, P., Cui, M.Z., 2000. Methyl diamantane index (MDI) as a maturity parameter for  
551 Lower Palaeozoic carbonate rocks at high maturity and overmaturity. *Org. Geochem.*  
552 31, 267-272.

553 Li, S., Hu, S., Cao, J., Wu, M., Zhang, D., 2012. Diamondoid Characterization in Condensate by  
554 Comprehensive Two-Dimensional Gas Chromatography with Time-of-Flight Mass  
555 Spectrometry: The Junggar Basin of Northwest China. *International Journal of*  
556 *Molecular Sciences* 13, 11399-11410.

557 Mansoori, G.A., de Araujo, P.L.B., de Araujo, E.S., 2012. *Diamondoid Molecules: With*  
558 *Applications in Biomedicine, Materials Science, Nanotechnology & Petroleum Science.*  
559 *World Scientific Publishing Co. Pte. Ltd, Singapore.*

560 Marchand, A.P., 2003. Diamondoid hydrocarbons - Delving into nature's bounty. *Science* 299,  
561 52-53.

562 Moldowan, J.M., Dahl, J., Zinniker, D., Barbanti, S.M., 2015. Underutilized advanced  
563 geochemical technologies for oil and gas exploration and production-1. The  
564 diamondoids. *J. Pet. Sci. Eng.* 126, 87-96.

565 Osawa, E., Engler, E.M., Godleski, S.A., Inamoto, Y., Kent, G.J., Kausch, M., Schleyer, P.V., 1980.  
566 Bridgehead reactivities of ethanoadamantane - bromination and solvolysis of  
567 bromides. *J. Org. Chem.* 45, 984-991.

568 Palu, T., Hall, L., Edwards, D., Grosjean, E., Rollet, N., Boreham, C., Buckler, T., Higgins, K.,  
569 Nguyen, D., Khider, K., 2017. Source Rocks and Hydrocarbon Fluids of the Browse  
570 Basin, AAPG|SEG 2017 International Conference & Exhibition, London.

571 Peters, K.E., Walters, C.C., Moldowan, J.M., 2007. The biomarker guide. Vol. 2. Biomarkers and  
572 isotopes in petroleum exploration and earth history. Cambridge University Press,  
573 Cambridge, UK.

574 Rowland, S.J., Scarlett, A., West, C., Jones, D., Frank, R., 2011a. Diamonds in the rough:  
575 identification of individual naphthenic acids in oil sands process water. *Environ. Sci.*  
576 *Technol.* 45, 3154-3159.

577 Rowland, S.J., West, C.E., Scarlett, A.G., Jones, D., Frank, R.A., 2011b. Identification of  
578 individual tetra- and pentacyclic naphthenic acids in oil sands process water by  
579 comprehensive two-dimensional gas chromatography/mass spectrometry. *Rapid*  
580 *Commun. Mass Spectrom.* 25, 1198-1204.

581 Schulz, L.K., Wilhelms, A., Rein, E., Steen, A.S., 2001. Application of diamondoids to distinguish  
582 source rock facies. *Organic Geochemistry* 32, 365-375.

583 Silva, R.C., Silva, R.S.F., de Castro, E.V.R., Peters, K.E., Azevedo, D.A., 2013. Extended  
584 diamondoid assessment in crude oil using comprehensive two-dimensional gas  
585 chromatography coupled to time-of-flight mass spectrometry. *Fuel* 112, 125-133.



586 Silva, R.S.F., Aguiar, H.G.M., Rangel, M.D., Azevedo, D.A., Aquino Neto, F.R., 2011.  
587 Comprehensive two-dimensional gas chromatography with time of flight mass  
588 spectrometry applied to biomarker analysis of oils from Colombia. *Fuel* 90, 2694-2699.

589 Spaak, G., 2017. *Molecular and Isotopic Perspectives on Australian Petroleum Systems:*  
590 *Hydrocarbon Fluid Correlations and Source Rock Depositional Environments in the*  
591 *Canning and Browse Basins (Doctoral dissertation). Curtin University, Perth.*

592 Spaak, G., Grice, K., Edwards, D.S., Scarlett, A.G., Grosjean, E., 2016. Poster presentation:  
593 Combining GCxGC and CSIA of diamondoids to unravel the sources of (biodegraded)  
594 hydrocarbons in the Browse Basin, 19th Australian Organic Geochemistry Conference,  
595 Fremantle, 4-7th December 2016.

596 Stout, S.A., Douglas, G.S., 2004. Diamondoid hydrocarbons - Application in the chemical  
597 fingerprinting of natural gas condensate and gasoline. *Environ. Forensics* 5, 225-235.

598 Tran, T.C., Logan, G.A., Grosjean, E., Ryan, D., Marriott, P.J., 2010. Use of comprehensive two-  
599 dimensional gas chromatography/time-of-flight mass spectrometry for the  
600 characterization of biodegradation and unresolved complex mixtures in petroleum.  
601 *Geochim. Cosmochim. Acta* 74, 6468-6484.

602 Volkman, J.K., Alexander, R., Kagi, R.I., Woodhouse, G.W., 1983. Demethylated hopanes in  
603 crude oils and their applications in petroleum geochemistry. *Geochim. Cosmochim.*  
604 *Acta* 47, 785-794.

605 Wang, Z., Stout, S.A., Fingas, M., 2006. Forensic Fingerprinting of Biomarkers for Oil Spill  
606 Characterization and Source Identification. *Environ. Forensics* 7, 105-146.

607 Wei, Z.B., Moldowan, J.M., Peters, K.E., Wang, Y., Xiang, W., 2007a. The abundance and  
608 distribution of diamondoids in biodegraded oils from the San Joaquin Valley:  
609 Implications for biodegradation of diamondoids in petroleum reservoirs. *Organic*  
610 *Geochemistry* 38, 1910-1926.

611 Wei, Z.B., Moldowan, J.M., Zhang, S.C., Hill, R., Jarvie, D.M., Wang, H.T., Song, F.Q., Fago, F.,  
612 2007b. Diamondoid hydrocarbons as a molecular proxy for thermal maturity and oil  
613 cracking: Geochemical models from hydrous pyrolysis. *Organic Geochemistry* 38, 227-  
614 249.

615 Wilde, M.J., Rowland, S.J., 2018. Naphthenic acids in oil sands process waters: Identification by  
616 conversion of the acids or esters to hydrocarbons. *Org. Geochem.* 115, 188-196.

617 Wingert, W.S., 1992. GC-MS analysis of diamondoid hydrocarbons in Smackover petroleum.  
618 *Fuel* 71, 37-43.

619 Zhang, S., Huang, H., Xiao, Z., Liang, D., 2005. Geochemistry of Palaeozoic marine petroleum  
620 from the Tarim Basin, NW China. Part 2: Maturity assessment. *Organic Geochemistry*  
621 36, 1215-1225.

622

623

624 **Table and Figure Legends**

625 *Tables*

626 Table 1: Locations and ages of Australian crude oils and condensates sampled

627 Table 2 Comparison of indices derived from 2,4-ethanoadamantanes and diamondoids

628

629 *Figures*

630 Fig. 1: Synthesis of 2,4-ethanoadamantane and mass spectra produced by (A) GC-MS  
631 (quadrupole mass spectrometer) and (B) GC×GC-TOFMS (time of flight mass  
632 spectrometer).

633 Fig. 2: Two dimensional gas chromatography elution positions of tetracyclic caged  
634 hydrocarbons (red squares) relative to diamondoids and *n*-alkanes. MA =  
635 methyladamantane, EA = ethyladamantane, MD = methyldiamantane, *n*C<sub>x</sub> = alkane  
636 carbon number.

637 Fig. 3: Peaks with mass spectra consistent with methyl (C1), dimethyl (C2) and  
638 trimethyl (C3) ethanoadamantanes present in the Cretaceous Cornea-1 oil. Some  
639 peaks were also present in other oils and condensates, and in the alkyldiamantane  
640 mixture.

641 Fig. 4: Linear regression of the ratio of the sum of methyladamantanes ( $\Sigma$ MA)/sum of  
642 methylethanoadamantanes ( $\Sigma$ ME) versus  $\Sigma$ MA/sum of methyldiamantanes ( $\Sigma$ MD).  
643 Closed black circles highlight biodegraded oils. Names of oils referred to in text are  
644 highlighted for reference.

645

646 Table 1 Locations and ages of Australian crude oils and condensates sampled

Well	Family*	Sample	Basin	Reservoir Age	Biodeg
Caswell-1	IV	Light oil	Browse	Cret.	N
Caswell-2	IV	Light oil	Browse	Cret.	N
Gwydion-1	IV	Oil	Browse	Cret.	Y
Cornea-1	IV	Oil	Browse	Cret.	Y
Focus-1	IV	Oil	Browse	Cret.	Y
Sparkle-1	IV	Oil	Browse	Cret.	Y
Cornea South	IV	Oil	Browse	Cret.	Y
Titanichthys-1	III	Condensate	Browse	L. Jura. – E. Cret.	N
Ichthys-1A	III	Condensate	Browse	L. Jura. – E. Cret.	N
Dinichthys-1	III	Condensate	Browse	L. Jura. – E. Cret.	N
Dinichthys North-1	III	Condensate	Browse	Jura.	N
Concerto-1	III	Condensate	Browse	Jura.	
Kronos-1	III	Condensate	Browse	Jura.	N
Prelude-1A	III	Condensate	Browse	L. Jura. – E. Cret.	N
Mimia-1	III	Condensate	Browse	L. Jura. – E. Cret.	N
Scott Reef-1	II	Condensate	Browse	Jura.	N

North Scott Reef-1	II	Condensate	Browse	Jura.	N
Calliance-1	II	Condensate	Browse	Jura.	N
Brecknock-2	II	Condensate	Browse	Jura.	N
Gorgonichthys-1	II	Condensate	Browse	Jura.	N
Montara	I	Light oil	Bonaparte	Jura.	N
Mardie		Oil	Carnarvon	Cret.	Severe (8)
Windalia		Oil	Carnarvon	Cret.	Mix
Barrow		Oil	Carnarvon	Cret.	N (0)
Rough Range		Oil	Carnarvon	Cret.	N (0)
Rankin-1		Oil	Carnarvon	Triassic	Mixed
Eaglehawk		Oil	Carnarvon	Triassic	Mixed
Tuna-4		Oil	Gippsland	Tertiary	Mod (3)
Lakes Entrance		Oil	Gippsland	Tertiary	Severe (7)

647 \*Family grouping by Geoscience Australia cluster analysis (Fig. S2). Cret. = Cretaceous; Jura = Jurassic; L. = Late; E. Early; Biodeg =  
648 biodegraded; Peters and Moldowan biodegradation scale, if previously reported (cited in text), given in parentheses, if not then typical  
649 indicators of biodegradation e.g. absence of *n*-alkanes, presence of unresolved complex mixture (UCM) indicated by Y = Yes or N = No

650

Table 2 Comparison of indices derived from 2,4-ethanoadamantanes and diamondoids

Oil well	MEI*	MAI	EAI	MDI	A/D	A/E	E/D	$\Sigma$ MA/ $\Sigma$ MD	$\Sigma$ MA/ $\Sigma$ ME*	$\Sigma$ ME*/ $\Sigma$ MD
Caswell-1	n/a	0.53	n/a	0.32	n/a	n/a	n/a	7.1	n/a	n/a
Caswell-2	n/a	0.56	n/a	0.31	n/a	n/a	n/a	5.7	n/a	n/a
Gwydion-1	0.73	0.69	0.47	0.40	5.19	5.01	1.03	7.2	4.6	1.6
Cornea-1	0.67	0.72	0.56	0.36	2.88	5.58	0.52	5.0	4.9	1.0
Focus-1	0.72	0.81	0.47	0.38	4.34	5.70	0.76	11.0	9.2	1.2
Sparkle-1	0.61	0.69	0.43	0.41	5.00	4.42	1.13	9.0	5.7	1.6
Cornea South	0.70	0.64	0.46	0.39	6.47	5.25	1.23	9.2	5.2	1.8
Titanichthys-1	0.76	0.63	0.33	0.38	5.81	3.94	1.47	10.5	6.8	1.6
Ichthys-1A	0.72	0.63	0.34	0.33	5.79	4.33	1.34	8.4	7.9	1.1
Dinichthys-1	0.77	0.63	0.34	0.31	5.23	3.90	1.34	9.0	6.6	1.4
Dinichthys N-1	0.73	0.75	0.47	0.37	8.06	6.25	1.29	12.4	7.3	1.7
Concerto-1	0.80	0.68	0.39	0.39	7.77	6.74	1.15	12.0	7.4	1.6
Kronos-1	0.67	0.69	0.47	0.48	5.78	6.75	0.86	9.4	6.7	1.4
Prelude-1A	0.75	0.67	0.33	0.33	7.01	4.88	1.44	10.9	6.7	1.6
Mimia-1	0.75	0.67	0.21	0.33	10.59	8.53	1.24	18.4	10.5	1.8
Scott Reef-1	n/a	0.71	0.42	0.41	5.70	5.68	1.00	10.0	7.4	1.4

N. Scott Reef-1	0.73	0.71	0.42	0.38	6.44	5.66	1.14	13.1	8.3	1.6
Calliance-1	0.80	0.70	0.42	0.40	6.83	4.62	1.48	11.3	7.8	1.4
Brecknock-2	0.83	0.72	0.43	0.41	6.36	5.62	1.13	12.3	8.5	1.4
Gorgonichthys-1	0.77	0.74	0.45	0.38	8.33	7.57	1.10	15.7	9.3	1.7
Montara	0.71	0.67	0.05	0.40	2.59	3.13	0.83	3.9	5.9	0.6
Mardie	0.58	0.63	0.74	0.48	0.30	0.32	0.93	0.7	0.7	1.1
Windalia	0.57	0.64	0.39	0.48	2.36	8.93	0.26	10.0	5.1	2.0
Barrow	0.74	0.70	0.19	0.47	5.37	3.84	1.40	18.2	13.8	1.3
Eaglehawk	0.64	0.66	0.46	0.52	n/a	1.23	n/a	8.5	6.3	1.4
Rankin	0.55	0.58	0.34	0.38	0.84	0.86	0.98	1.8	1.8	1.0
Roughrange	n/a	0.69	0.24	n/a	3.43	2.58	1.33	2.0	4.6	0.4
Lakes entrance	0.61	0.63	0.35	0.48	3.91	2.16	1.81	4.8	5.1	0.9
Tuna4	n/a	0.64	0.31	0.67	2.07	2.64	0.78	9.3	4.0	2.3

MEI = Methyl Ethanoadamantane Index:  $\Sigma(6\text{-ME} + 1\text{-ME} + 2\text{-ME})/\Sigma\text{Total methylethanoadamantanes (ME)}$

MAI = Methyl Adamantane Index:  $1\text{-MA}/(1\text{-MA} + 2\text{-MA})$

EAI = Ethyl Adamantane Index:  $1\text{-EA}/(1\text{-EA} + 2\text{-EA})$

MDI = Methyl Diamantane Index:  $4\text{-MD}/(1\text{-MD} + 3\text{-MD} + 4\text{-MD})$

A/D = Adamantane/Diamantane

A/E = Adamantane/Ethanoadamantane

E/D = Ethanoadamantane/Diamantane

$$\Sigma MA/\Sigma MD = (1-MA + 2-MA)/(1-MD + 3-MD + 4-MD)$$

$$\Sigma MA/\Sigma ME = (1-MA + 2-MA)/(6-ME + 1-ME + 2-ME)$$

$$\Sigma ME/\Sigma MD = (6-ME + 1-ME + 2-ME)/1-MD + 3-MD + 4-MD)$$

n/a = not applicable e.g. due to undetected peaks

\*Note that methylethanoadamantane assignment tentative

Author's Accepted Manuscript



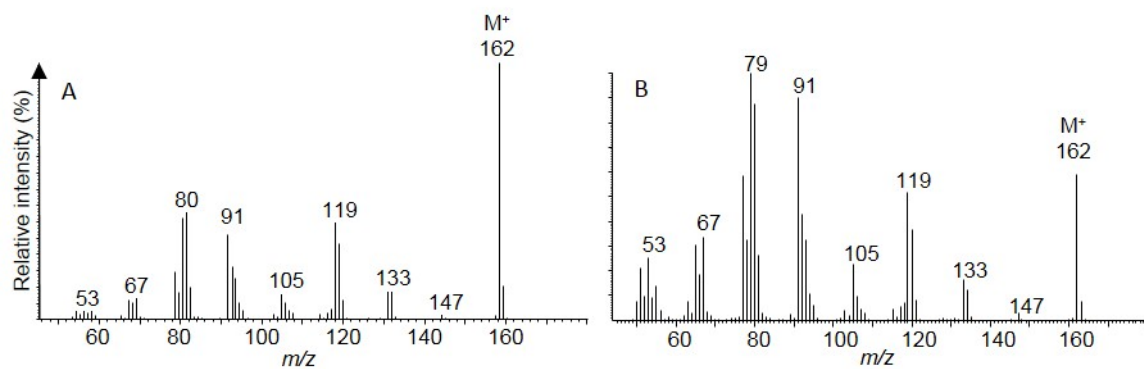
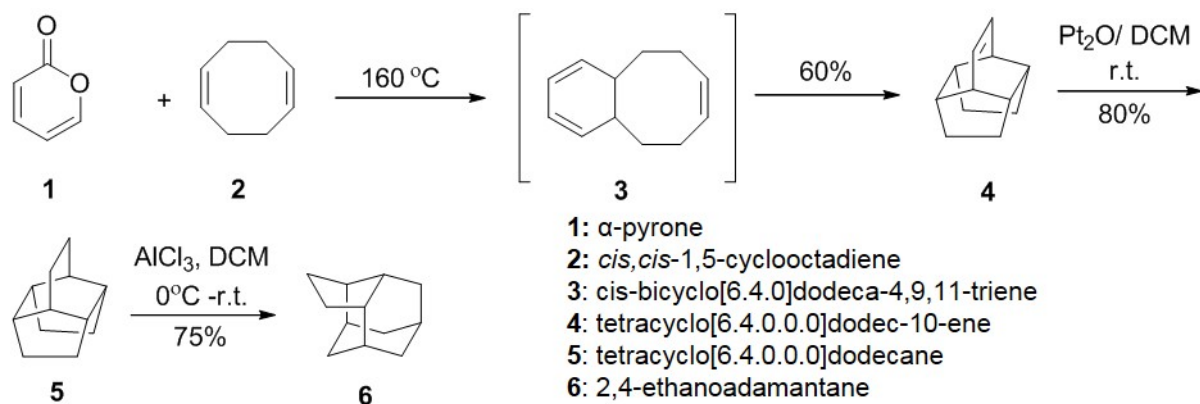


Fig. 1: Synthesis of 2,4-ethanoadamantane and mass spectra produced by (A) GC-MS (quadrupole mass spectrometer) and (B) GC $\times$ GC-TOFMS (time of flight mass spectrometer).

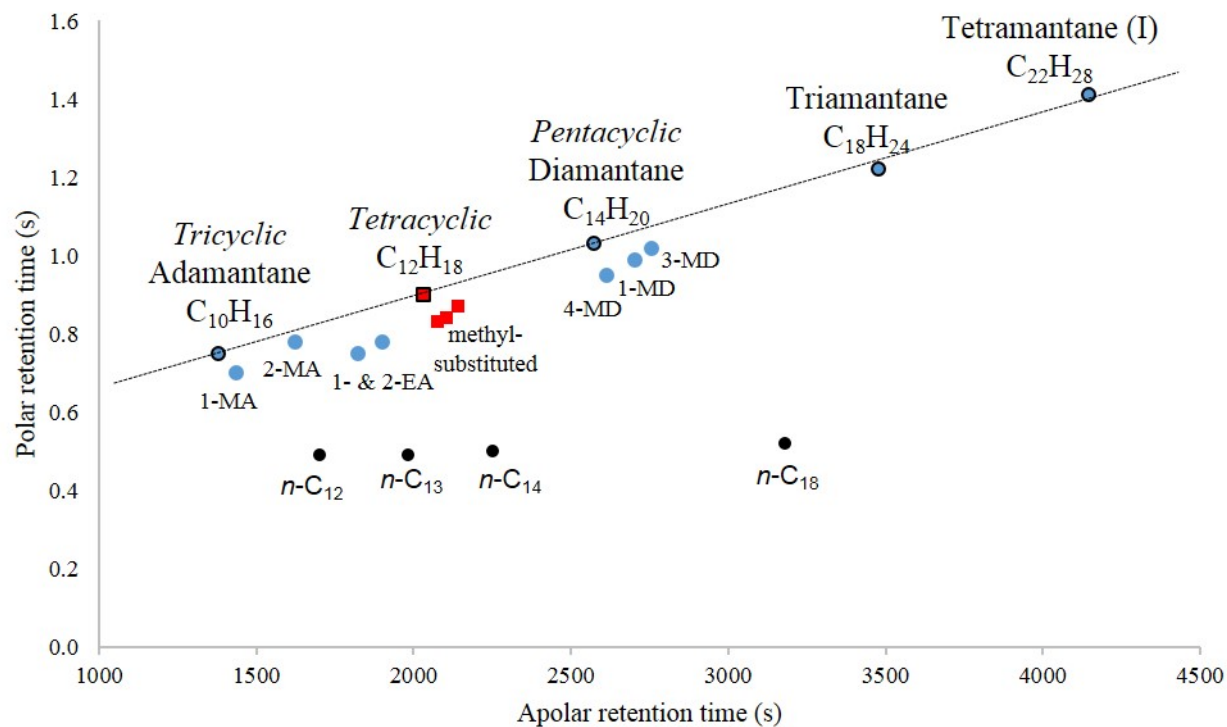


Fig. 2: Two dimensional gas chromatography elution positions of tetracyclic caged hydrocarbons (red squares) relative to diamondoids and *n*-alkanes. MA = methyladamantane, EA = ethyladamantane, MD = methyldiamantane, *n*C<sub>x</sub> = alkane carbon number.

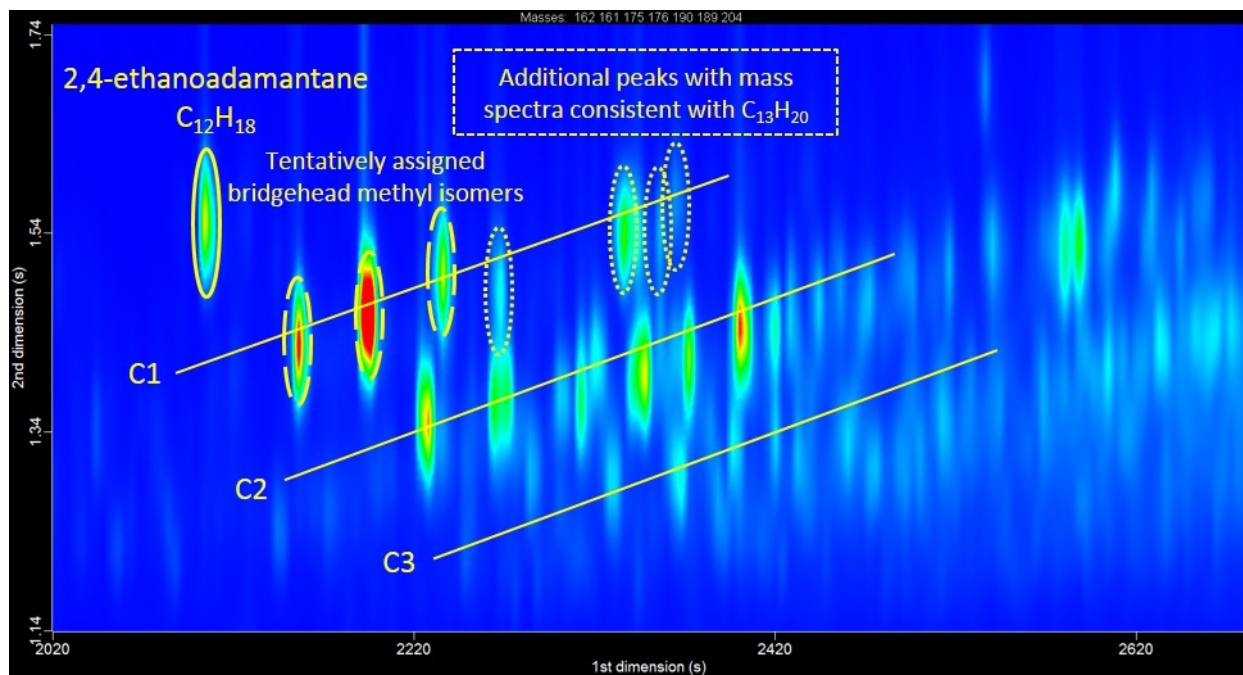


Fig. 3: Peaks with mass spectra consistent with methyl (C1), dimethyl (C2) and trimethyl (C3) ethanoadamantanes present in the Cretaceous Cornea-1 oil. Some peaks were also present in other oils and condensates, and in the alkyldiamantane mixture.

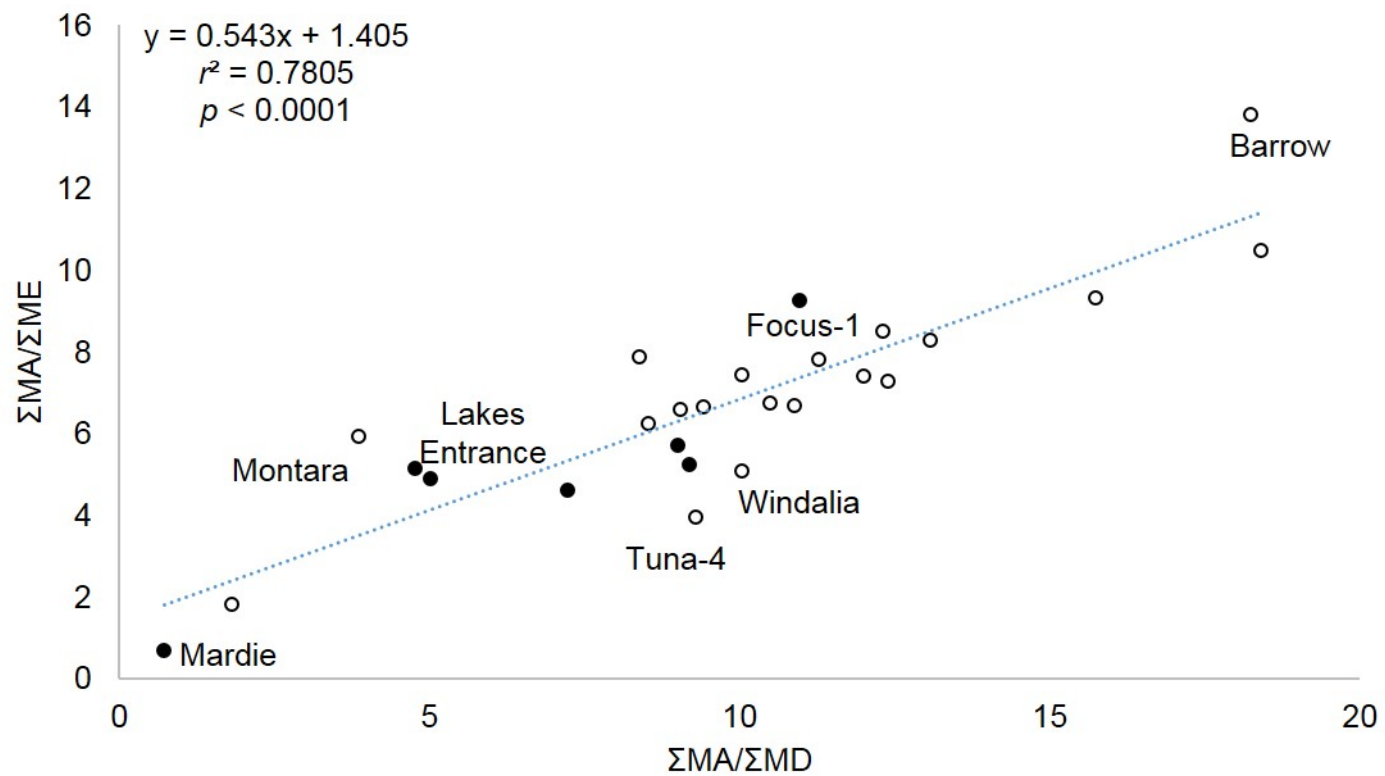


Fig. 4: Linear regression of the ratio of the sum of methyladamantanes ( $\Sigma MA$ )/sum of methylethanoadamantanes ( $\Sigma ME$ ) versus  $\Sigma MA$ /sum of methyladamantanes ( $\Sigma MD$ ). Closed black circles highlight biodegraded oils. Names of oils referred to in text are highlighted for reference.

## Supplementary Information

Title: Comparison of tri-, tetra- and pentacyclic caged hydrocarbons in Australian crude oils and condensates

Authors: Alan G. Scarlett<sup>a\*</sup>, Gemma Spaak<sup>a1</sup>, Shifaza Mohamed<sup>b</sup>, Chloé Plet<sup>a2</sup>, Kliti Grice<sup>a\*</sup>

<sup>a</sup>Western Australian Organic and Isotope Geochemistry Centre, The Institute for Geoscience Research, School of Earth and Planetary Sciences, Curtin University, Western Australia

<sup>b</sup> School of Pharmacy and Biomedical Sciences, Curtin University, Western Australia

\*Corresponding authors: [Alan.Scarlett@curtin.edu.au](mailto:Alan.Scarlett@curtin.edu.au) and [K.Grice@curtin.edu.au](mailto:K.Grice@curtin.edu.au)

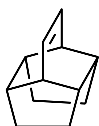
<sup>1</sup>Present address: Deltares, Subsurface and Groundwater Systems, Daltonlaan 600, 3584 BK Utrecht, the Netherlands

<sup>2</sup>Present address: CSIRO Mineral resources, Kensington, WA, 6151, Australia

## Synthesis of 2,4-ethanoadamantane

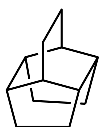
### Experimental

#### 1. Tetracyclo[6.4.0.0.0]dodec-10-ene (**4**)



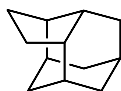
A mixture of *cis,cis*-1,5-cyclooctadiene (0.5 mL) and  $\alpha$ -pyrone (0.1 mL, 1.0 mmol) was heated under reflux for 24 h. The reaction mixture was then diluted with DCM (20 ml) and absorbed on to silica gel. The material was then purified by flash column chromatography to yield tetracyclo[6.4.0.0.0]dodec-10-ene **4** (0.1 g, 60%) as a white powder.  $^1\text{H}$  NMR ( $\text{CDCl}_3$ , 400 MHz): 6.20 (dd, 2H,  $J = 3.5$  Hz,  $J = 4.8$  Hz), 2.22-2.15 (m, 2H), 1.76-1.67 (m, 4H), 1.50-1.40 (m, 4H);  $^{13}\text{C}$  NMR ( $\text{CDCl}_3$ , 100 MHz): 131.1, 42.7, 40.2, 25.8; [GC-MS]: 160 m/z

#### 2. Tetracyclo[6.4.0.0.0]dodecane (**5**)



A solution of compound **4** (80 mg, 0.5 mmol) and catalytic amount of platinum oxide (approx. 10 mg) in anhydrous DCM (10 mL) was stirred under a hydrogen atmosphere for 24 h. The reaction mixture was filtered over a pad of celite and concentrated under reduced pressure to obtain tetracyclo[6.4.0.0.0]dodecane **5** (65 mg, 80%) as a yellowish powder. The crude material was used without further purification.  $^1\text{H}$  NMR ( $\text{CDCl}_3$ , 400 MHz): 2.02-1.92 (m, 3H), 1.68-1.59 (m, 9H), 1.27-1.56 (m, 6H); [GC-MS]: 162 m/z.

#### 3. 2,4-ethanoadamantane (**6**)



A solution of tetracyclo[6.4.0.0.0]dodecane **5** in anhydrous DCM (5 mL) was added dropwise to a stirred cooled (0 °C) suspension of pulverized aluminium chloride (1.5 g) in anhydrous DCM (10 mL) under an inert atmosphere. The reaction mixture was then brought up to r.t. and stirred for 1 h. The

reaction mixture was then cooled to 0 °C and water was added dropwise to decompose the AlCl<sub>3</sub>. The organic layer was then extracted, dried (MgSO<sub>4</sub>) and concentrated under reduced pressure to yield 2,4-ethanoadamantane **6** (49 mg, 75%). The isolated material did not require purification. <sup>13</sup>C NMR (CDCl<sub>3</sub>, 100 MHz): 42.0, 39.6, 37.1, 33.3, 32.1, 29.6, 26.7; [GC-MS]: 162 m/z.

Table S1 Molecular properties and calculated energies of tri-, tetra- and pentacyclic caged hydrocarbons computed using Spartan '16 version 2.0.7 (Wavefunction Inc, Irvine, CA). Strain energies were calculated using the program settings 'Molecular mechanics'; total energies and thermodynamic properties were calculated using 'Equilibrium Geometry' at ground state with 'Density Functional'  $\omega$ B97X-D and 6-31G\*.

Molecule	Formula	Mol Wt. (amu)	Energy (total) (au)	Energy (strain) (kJ/mol)	ZPE kJ/mol	H <sup>o</sup> (au)	Cv (J/mol.K)	S <sup>o</sup> (J/mol.K)	G <sup>o</sup> (au)
Adamantane (A)	C <sub>10</sub> H <sub>16</sub>	136.238	-390.627	74.35	649.20	-390.372	133.60	340.10	-390.411
1-MA	C <sub>11</sub> H <sub>18</sub>	150.265	-429.935	108.94	722.14	-429.651	159.09	365.31	-429.692
2-MA	C <sub>11</sub> H <sub>18</sub>	150.265	-429.931	100.44	725.04	-429.646	155.61	363.68	-429.687
Iceane (I)	C <sub>12</sub> H <sub>18</sub>	162.276	-468.012	202.71	748.16	-467.719	153.46	346.26	-467.758
1-MI	C <sub>13</sub> H <sub>20</sub>	176.303	-507.320	240.21	823.08	-506.997	176.96	374.30	-507.040
2-MI	C <sub>13</sub> H <sub>20</sub>	176.303	-507.310	252.99	823.14	-506.987	176.66	382.12	-507.030
Ethanoadamantane (E)	C <sub>12</sub> H <sub>18</sub>	162.276	-468.023	162.12	746.44	-467.730	155.33	358.65	-467.770
6-ME	C <sub>13</sub> H <sub>20</sub>	176.303	-507.328	211.22	820.22	-507.005	180.37	382.18	-507.049
1-ME	C <sub>13</sub> H <sub>20</sub>	176.303	-507.330	199.61	819.05	-507.008	181.27	384.21	-507.052
2-ME	C <sub>13</sub> H <sub>20</sub>	176.303	-507.329	203.03	820.02	-507.007	180.56	382.71	-507.050
Diamantane (D)	C <sub>14</sub> H <sub>20</sub>	188.314	-545.445	156.03	842.67	-545.115	176.92	374.12	-545.157
4-MD	C <sub>15</sub> H <sub>20</sub>	202.341	-584.750	203.07	917.01	-548.390	201.35	396.80	-584.435
1-MD	C <sub>15</sub> H <sub>20</sub>	202.341	-584.750	203.03	916.99	-584.390	201.50	397.14	-584.435
3-MD	C <sub>15</sub> H <sub>20</sub>	202.341	-584.748	182.30	917.78	-584.390	200.08	399.17	-584.434

M = methyl

amu = atomic mass units

au = atomic units (1 atomic unit = 2625 kJ/mol)

ZPE = Zero point energy

H<sup>o</sup> = enthalpy

Cv = Heat capacity at constant volume

S<sup>o</sup> = Entropy (note that calculations are problematic in part due to the harmonic approximation.)

G<sup>o</sup> = Gibbs free energy

Table S2 Concentrations ( $\mu$ g/g oil) of tri-, tetra- and pentacyclic caged hydrocarbons in a range of Australian crude oils and condensates



Oil well	A	1-MA	2-MA	E	1-ME*	6-ME*	2-ME*	D	4-MD	1-MD	3-MD
Caswell-1	144	500	443	0	0	0	0	0	42	55	36
Caswell-2	118	487	378	0	0	0	0	0	48	60	44
Gwydion-1	3914	10485	4766	781	864	1817	634	754	847	670	589
Cornea-1	4792	11745	4575	859	977	1804	560	1666	1179	1208	863
Focus-1	2645	14327	3446	464	535	1076	312	609	608	578	432
Sparkle-1	1629	5996	2646	369	365	909	243	326	393	315	250
Cornea South	1526	4100	2324	291	311	718	198	236	271	233	195
Titanichthys-1	286	959	563	73	47	118	60	49	55	42	48
Ichthys-1A	203	571	342	47	0	75	41	35	36	35	38
Dinichthys-1	259	839	489	66	52	102	47	49	46	50	51
Dinichthys N-1	1020	3361	1110	163	138	367	108	127	132	115	114
Concerto-1	615	1785	843	91	92	187	75	79	86	68	65
Kronos-1	1387	3610	1593	206	194	430	156	240	264	152	137
Prelude-1A	309	886	508	63	54	100	54	44	42	45	41
Mimia-1	996	3171	1542	117	110	260	79	94	84	89	83
Scott Reef-1	827	2687	1099	146	129	270	110	145	153	112	112
N. Scott Reef-1	825	2996	1228	146	129	270	110	128	122	103	98
Calliance-1	496	1851	777	107	82	174	80	73	93	72	68
Brecknock-2	585	2109	833	104	93	185	68	92	98	73	68
Gorgonichthys-1	907	3726	1281	120	138	298	101	109	121	99	98
Montara	755	2714	1345	241	192	398	93	291	422	380	249
Mardie	25	132	77	78	87	153	69	84	137	90	58
Windalia	166	779	446	19	63	137	41	70	58	38	26
Barrow	252	1037	441	66	37	48	22	47	38	26	17

Eaglehawk	383	2092	1074	148	128	288	90	112	192	87	92
Rankin	54	255	188	63	58	145	41	64	94	83	68
Roughrange	9	48	22	7	5	10	0	0	5	4	26
Lakes entrance	303	1536	891	115	113	271	89	147	244	156	109
Tuna4	119	476	258	55	57	102	26	30	22	24	33

---

Adamantane (A), 2,4-ethanoadamantane (E), Diamantane (D) and their methyl-substituted isomers (M).

\*carbon numbers of methyl isomers of ethanoadamantane tentatively assigned.

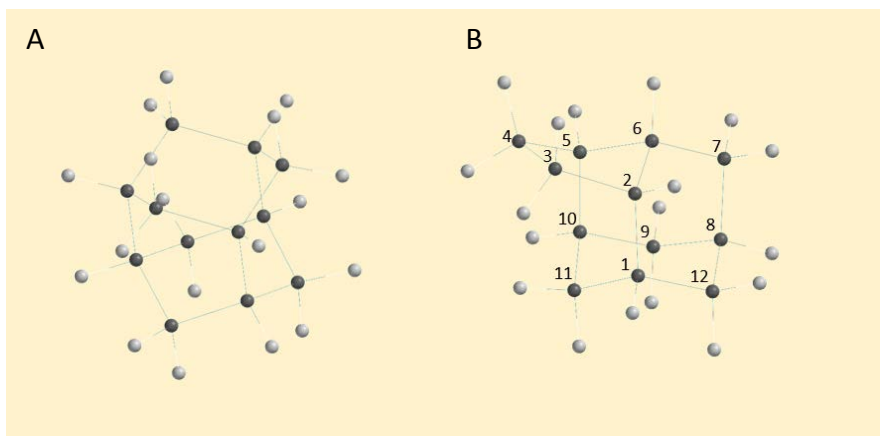


Fig. S1. Chemical structures of iceane (A) and 2,4-ethanoadamantane showing bridgehead positions at 1, 2, 6 and 8 (B).

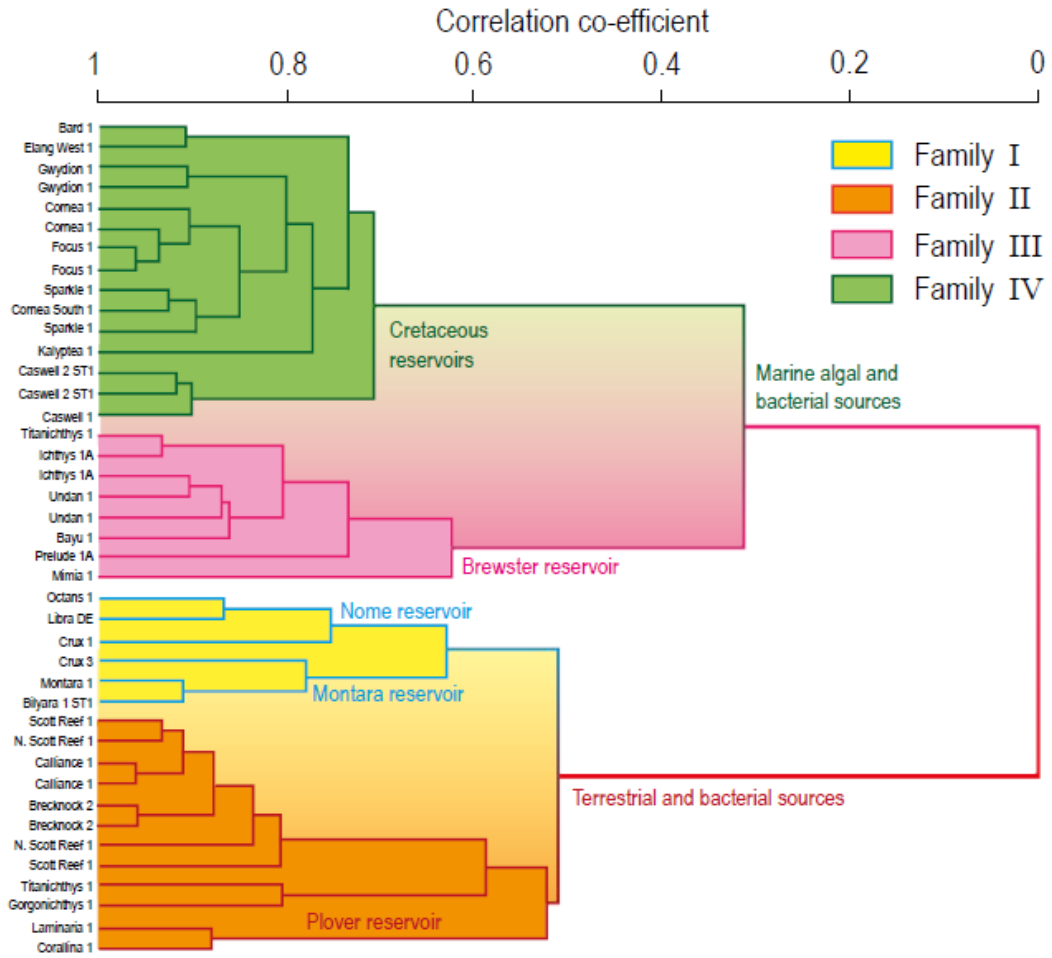


Fig. S2: Dendrogram comparing Browse Basin fluid families with those of selected samples from the Bonaparte Basin based mainly on  $^{13}\text{C}$  of saturates and aromatics, tri- and tetracyclic terpanes and sterane biomarkers (after Edwards et al., 2016).

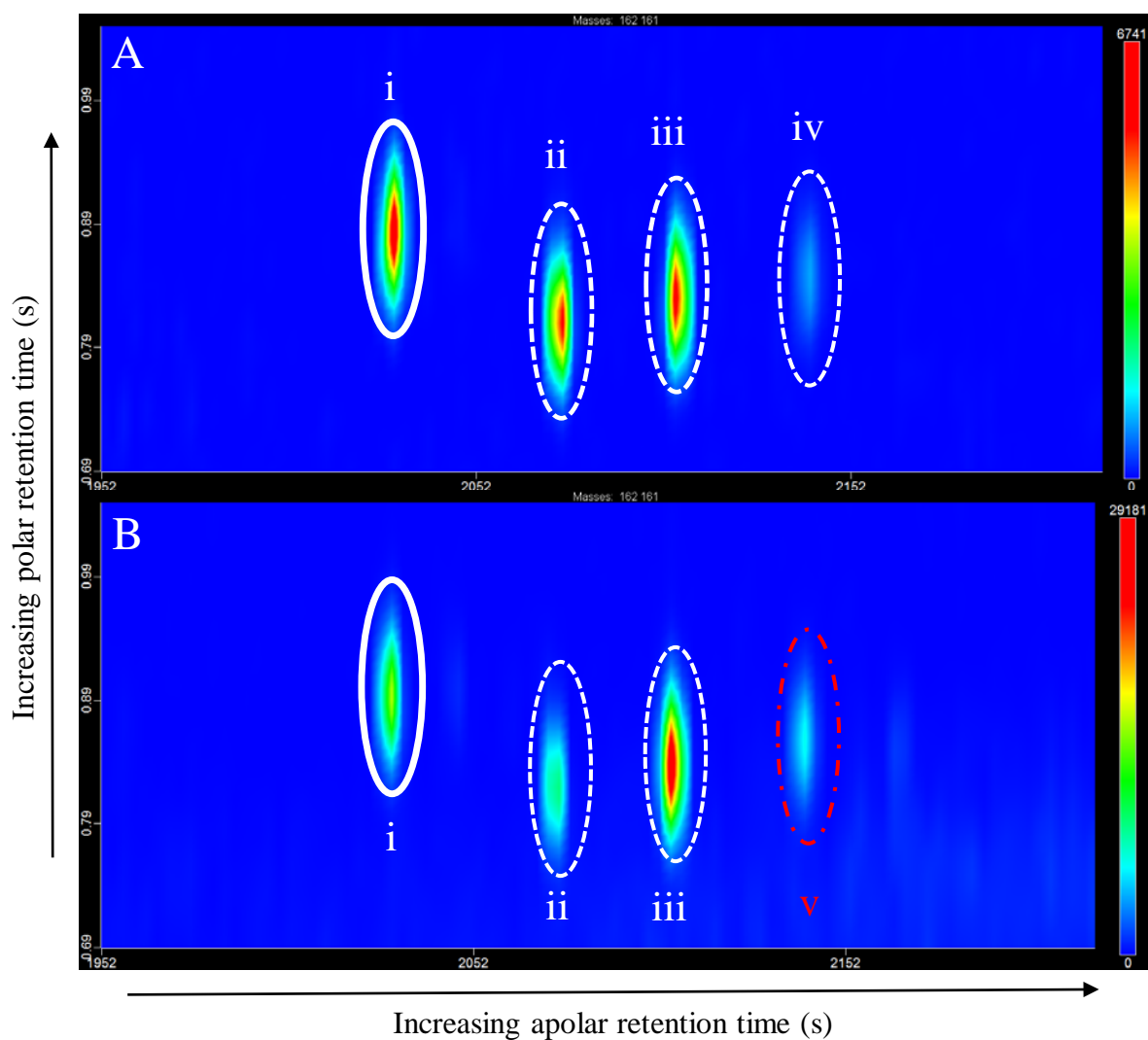


Fig. S3. GCxGC-TOFMS chromatograms of elution region of tetracyclic caged hydrocarbons in alkyladamantane mixture (A) and biodegraded Mardie crude oil (B). Peak i is the parent structure  $C_{12}H_{18}$  with molecular ion  $m/z$  162 (Figure S4A) and peaks ii – v correspond to methyl substituted structure with molecular ion  $m/z$  176. Peaks i – iii in (A) and (B) have identical mass spectra but iv and v are clearly different (Figure S5).

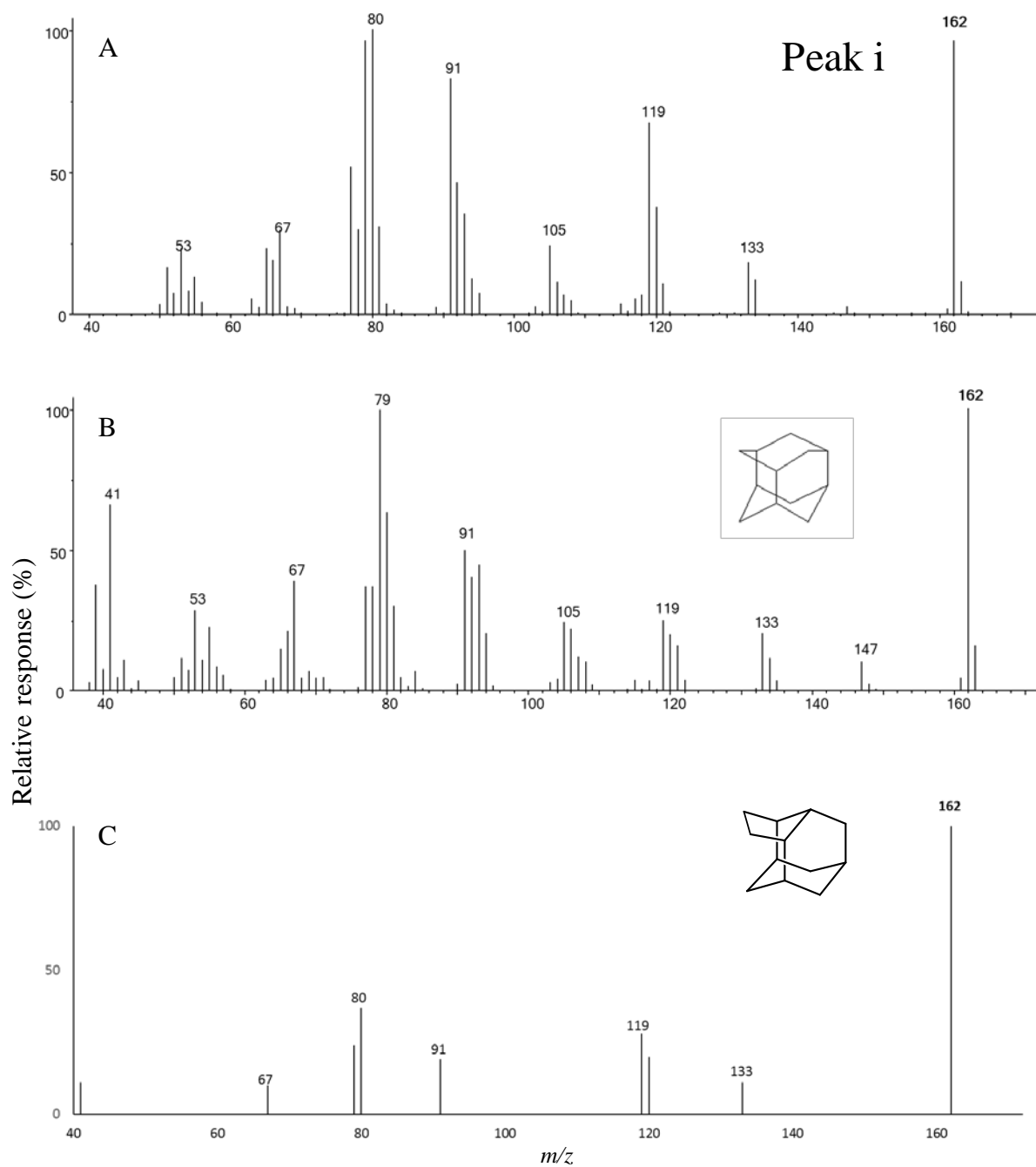


Fig. S4. Time-of-flight mass spectrum for unknown peak (Figure S3 peak i) in alkyldiamantane mixture consistent with  $C_{12}H_{18}$  tetracyclic hydrocarbon (A), unspecified mass spectrum in NIST library for iceane (B) and unspecified mass spectrum of 2,4-ethanoadamantane reproduced from Hála et al. (1966) (C).

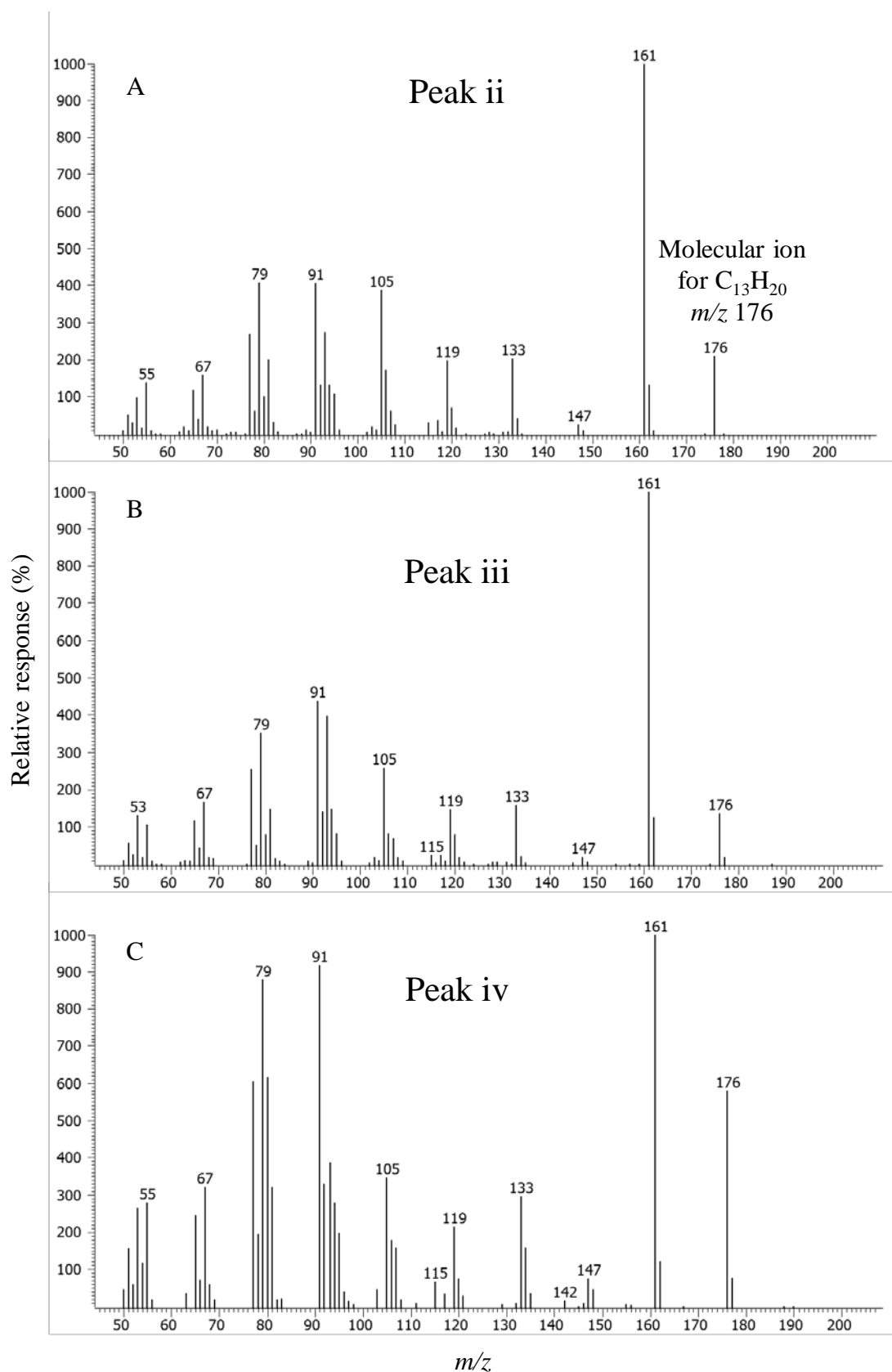


Fig. S5. Time-of-flight mass spectra for peaks (corresponding to ii – iv in Fig. S3) consistent with methyl-substituted isomers of  $C_{12}H_{18}$  caged tetracyclic hydrocarbons in alkyl-diamantane mixture.

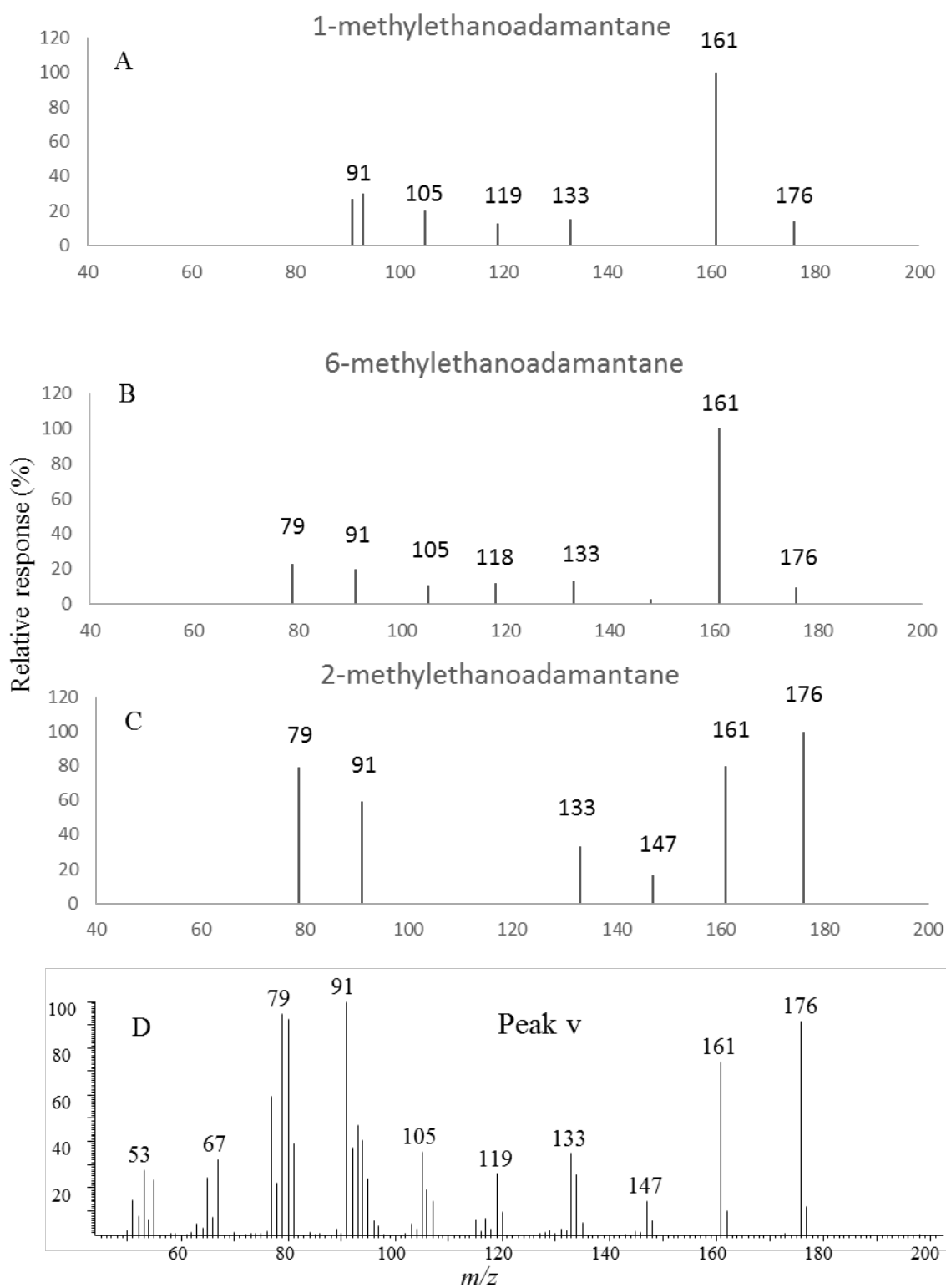


Fig. S6. Mass spectra reproduced from Osawa et al (1980) for 1-methylethanoadamantane (A), 6-methylethanoadamantane (B) and 2-methylethanoadamantane (C), and time-of-flight mass spectrum of peak v observed in many oils eluting at the same 2D times as peak iv in alkyladamantane mixture (see Fig. S3 and S5).



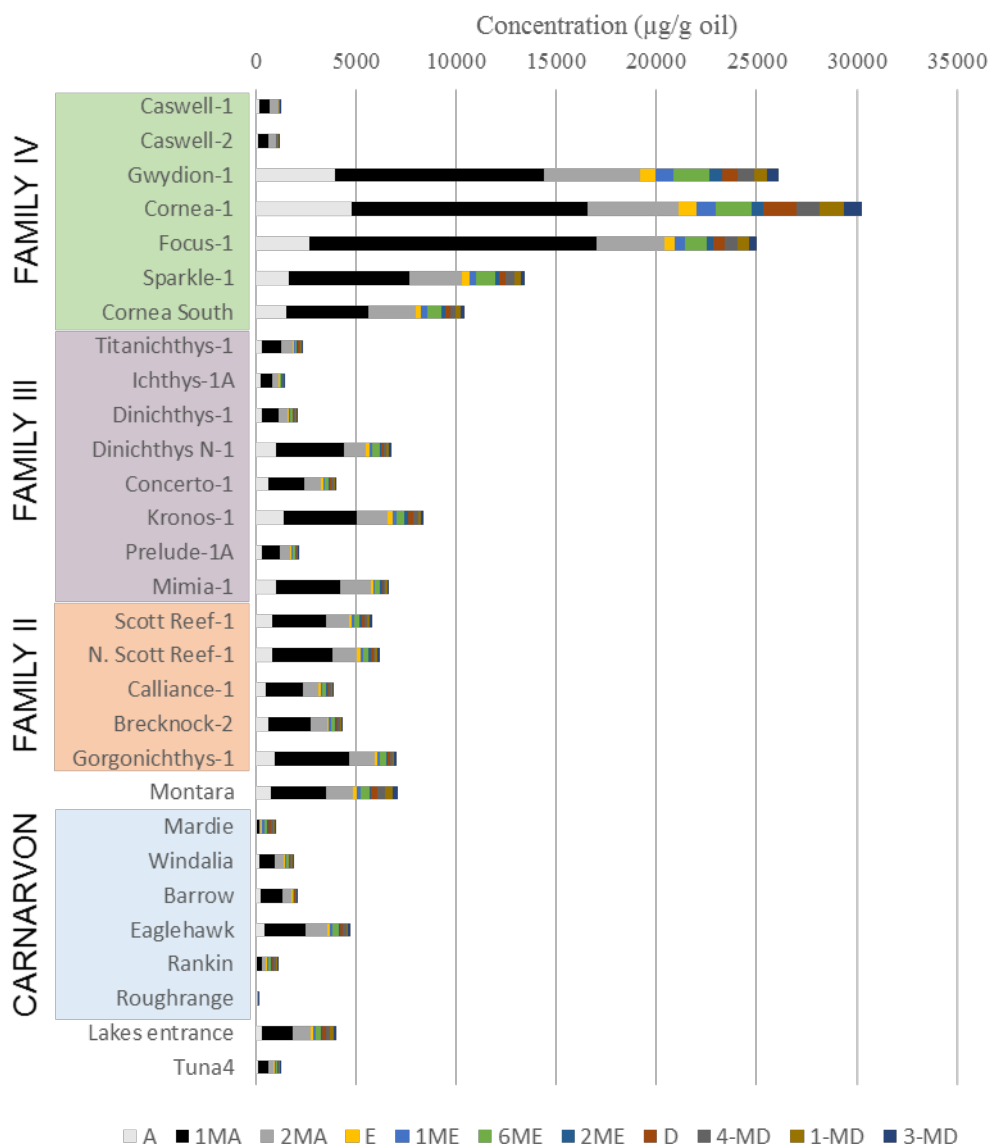


Fig. S7. Relative concentrations of adamantane (A), ethanoadamantane (E) and diamantane (D) plus their methyl substituted isomers numbered by carbon substitution position e.g. 4-MD = 4-methyldiamantane. Families II, III and IV refer to Browse basin groupings in dendrogram Fig. S2. The Carnarvon basin oils are related but of varying biodegradation levels. Montara is a light oil from the Bonaparte basin and Tuna4 and Lakes Entrance are from Gippsland (Table 1).

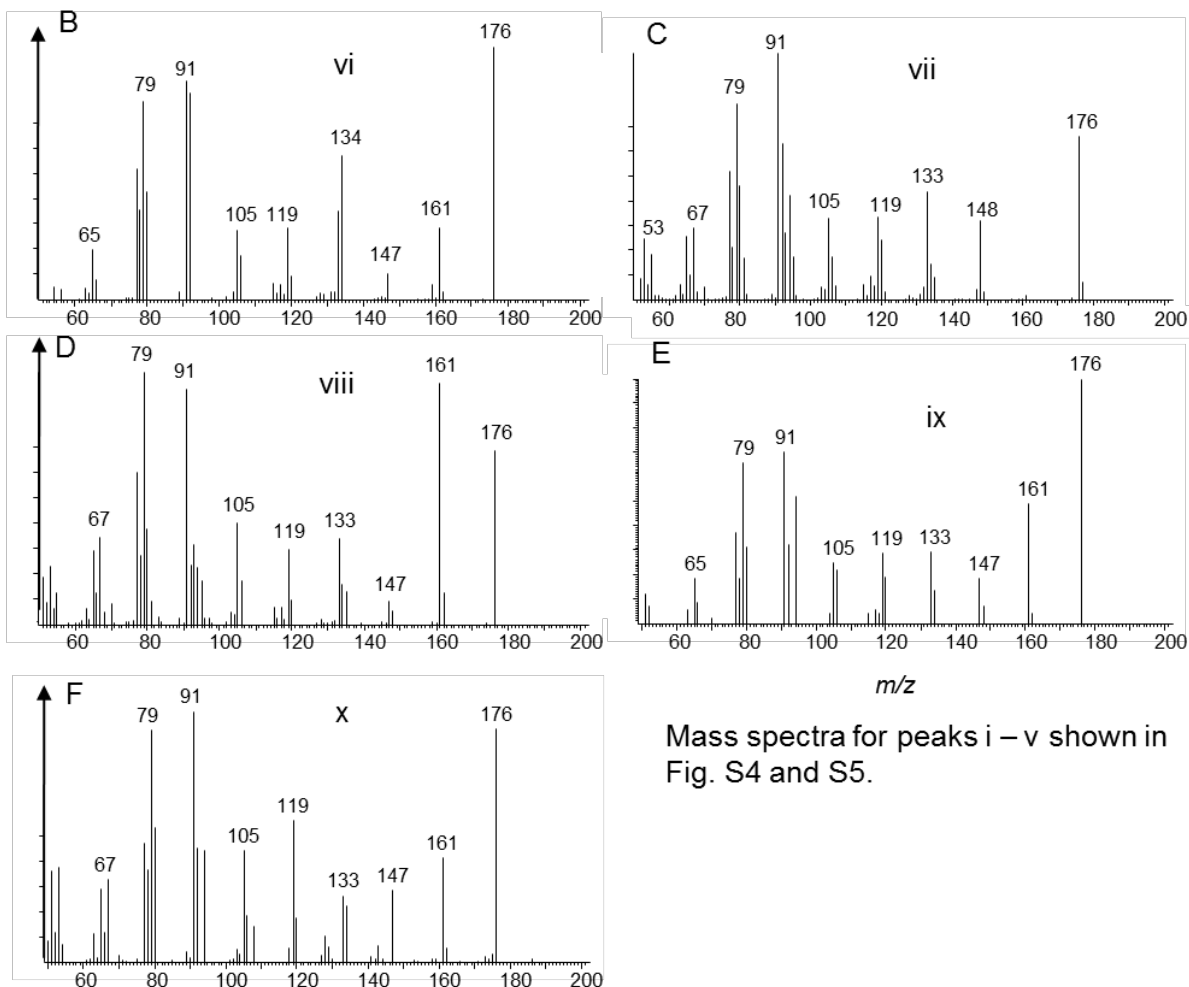
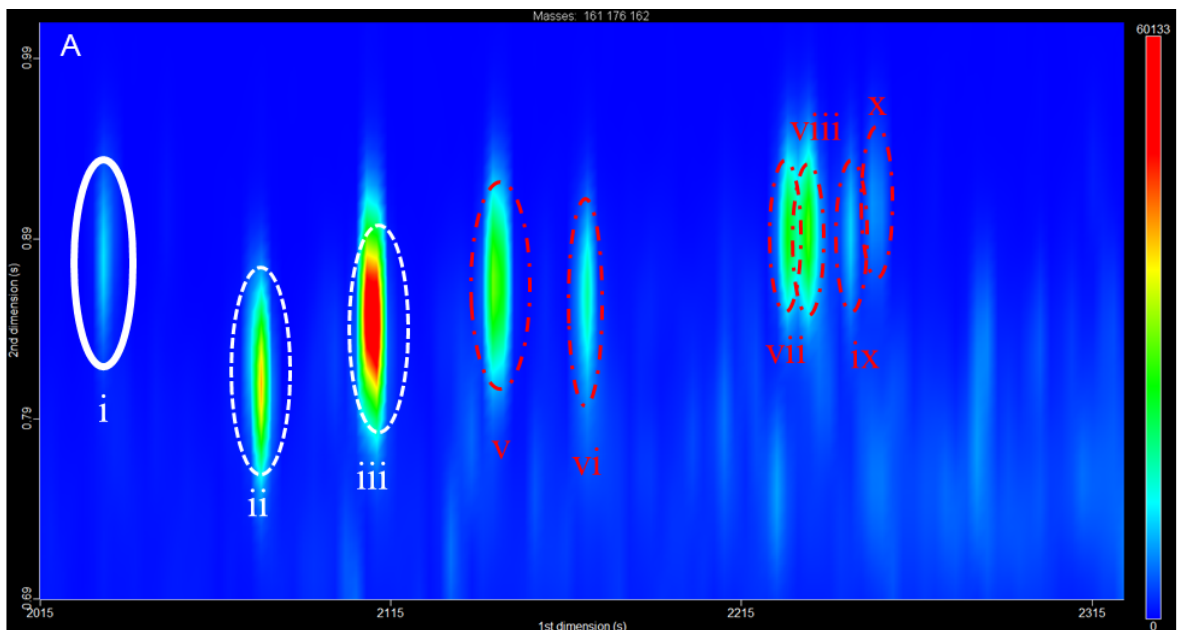


Fig. S8 GCxGC-TOFMS extracted ion chromatogram ( $m/z$  161, 162, 176) of Lakes Entrance oil (A) showing elution positions of 2,4-ethanoadamantane (i) and possible methyl isomers ii – x with mass spectra corresponding to peaks vi – x (B – F) observed more prominently in biodegraded oils and condensates.

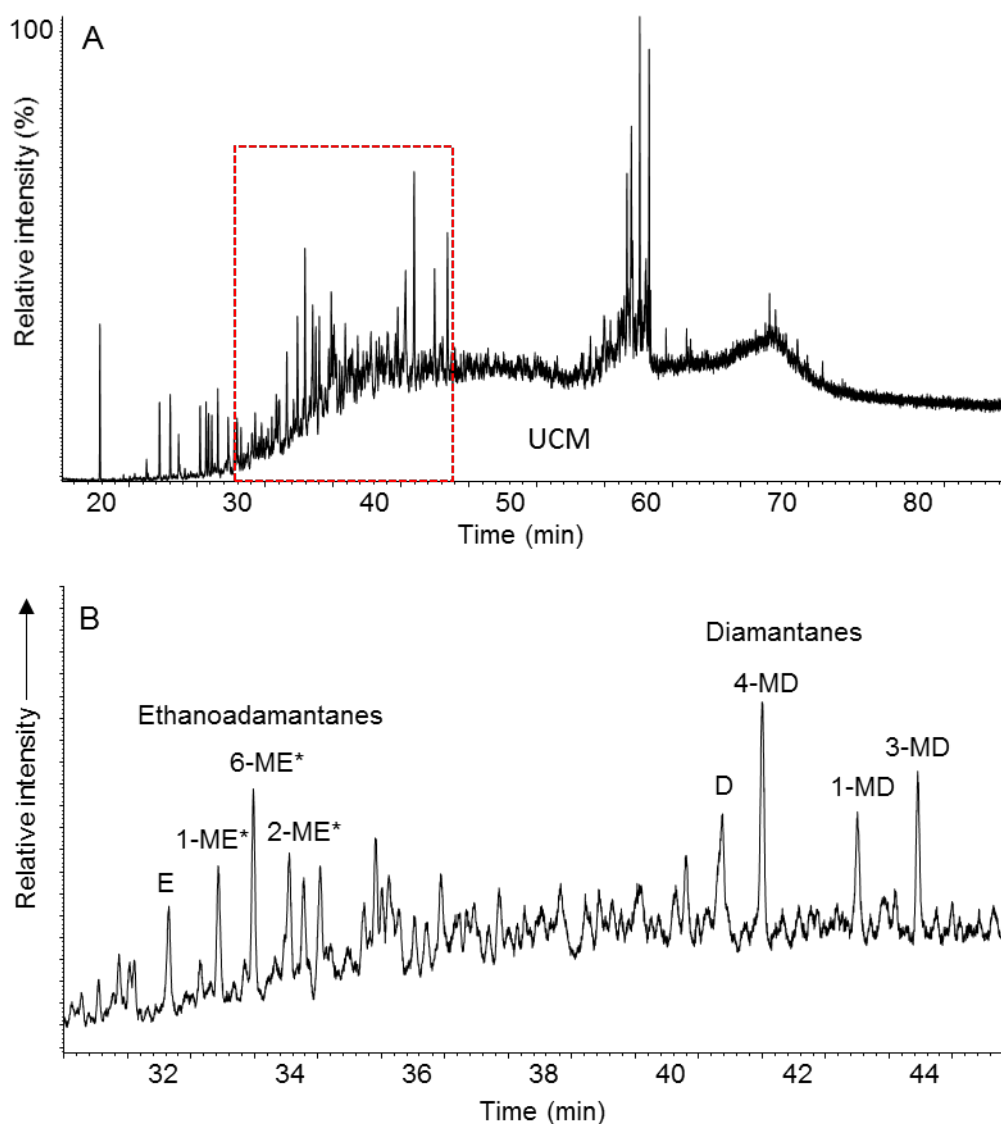


Fig. S9. GC-MS Selected Ion Monitoring chromatogram (A) with zoomed in region highlighted by red box (B) showing peaks ethanoadamantane (E) and tentatively assigned methyl isomers (ME) substituted at the 1-, 6- and 2- bridgehead positions. Also shown are diamantane (D) its methyl isomers 4-MD, 1-MD and 3-MD. Ions monitored were  $m/z$  162, 161 and 176 for ethanoadamantanes,  $m/z$  188, 187 and 202 for diamantanes.